Propulsion Devices for Locomotion at Low-Reynolds Number

by

Brian Chan

Submitted to the Department of Mechanical Engineering
in partial fulfillment of the requirements for the degree of

Master of Science

at the

MASSACHUSETTS INSTITUTE OF TECHNOLOGY

June 2004

Author .....
Department of Mechanical Engineering
May 7, 2004

Certified by .....
Anette Hosoi
Assistant Professor
Thesis Supervisor

Accepted by .....
Ain A. Sonin
Chairman, Department Committee on Graduate Students

Propulsion Devices for Locomotion at Low-Reynolds Number

by

Brian Chan

Submitted to the Department of Mechanical Engineering
on May 7, 2004, in partial fulfillment of the
requirements for the degree of
Master of Science

Abstract

We have designed, built, and tested three novel devices that use low-Reynolds number flows for self propulsion. The three-link swimmer is designed to swim through in a free viscous fluid using cyclic flipping motion of two rigid fins attached to a rigid midsection. Robosnail 1 uses lubrication pressures underneath a flexible, sinusoidally waving boundary to generate thrust, and Robosnail 2 uses five independently controlled translating feet segments to move on a layer of 8 percent Laponite, a shear thinning clay suspension which gives it the ability to adhere to and scale inclines and inverted surfaces. The three link swimmer was found to travel up to 0.034 body lengths per four-stroke cycle, Robosnail 1 was found to move at a speed of roughly half the wave speed of the foot (measured with respect to the snail), a result consistent for wave speeds between 0 and 2 cm/s. Robosnail 2 was able to move forward at all inclines from zero to 180 degrees inverted, with back-slip ranging from 40 to 80 percent.

Thesis Supervisor: Anette Hosoi
Title: Assistant Professor

Acknowledgments

The author would like to thank Benjamin Dupuy, Susan Ji, Catherine Koveal, David Hu, John Bush, Gareth McKinley, Christian Claasen, Todd Thorsen, and Mats Cooper.

Contents

List of Figures

Chapter 1

Introduction

The rising popularity of microfluidic devices invites the researcher to explore new methods of transporting fluids and things through fluids. Large scale fluid machinery is most often composed of rotating components like propellers. Up to date the most studied low-Re propulsion method is still the rotating flagella, which can be the low-Re analog of the propeller. A working version of the flagella swimmer was built by G.I. Taylor in the 50s. However, there are many other possible ways to move at low Reynolds Number.

We have designed, built and tested three novel machines for moving at low Reynolds number: the three-link swimmer, and two mechanical snails modeled after real snails. The simple prototypes may serve as the basic foundation for new robot designs. While two of the devices still utilize rotary mechanisms (motor and gearboxes) to drive the motion of non-rotary parts, rotation is not essential to the functionality of the devices, as they could conceivably be actuated with non-rotary actuators.

The low-Reynolds number regime ($Re \ll 1$) encompasses very small organisms and devices moving in highly viscous fluids. In this regime, all machines exhibiting time-reversible motions are unable to experience a net displacement. Organisms and machines designed to operate at low Re must therefore use motion that is not purely reciprocal.

The concept of the three link swimmer was described by E.M. Purcell in his talk "Life at Low Reynolds Number"[11] It is is arguably the simplest low-Re swimmer.

Since a two link swimmer is only capable of a reversible cyclic motion, its net translation is oscillatory about a fixed point. We have designed the first working prototype of this device and have done fluid tests to confirm its direction of motion.

We have built two mechanical snails, Robosnail 1 and Robosnail 2: Each uses a different mechanism to move on a thin layer of viscous fluid. Robosnail 1 uses a bendable flapping sheet over a viscous Newtonian fluid. Lubrication pressures generated by the moving boundary propel the snail. Robosnail 2 uses a compressible sliding sheet on a layer of Laponite, a non-Newtonian, finite-yield stress fluid with characteristics similar to snail mucus. Solidified Laponite keeps the snail from slipping while a compression wave propagates along the foot, generating a net displacement. As the system is similar to the adhesive locomotion of land-snails, we will test the wall and ceiling climbing ability of the Robosnail 2.

The experiments will be used to confirm the results of numerical and theoretical models. Experimental relationships between prescribed physical parameters and motion will be drawn. These data may be helpful to inspire the design of similar low-Re machines.

Chapter 2

Theory

2.1 Stokes Flow

At very Low Reynolds number, the Navier-Stokes Equations reduce to the Stokes Equations. The Stokes equations are:

$$-\frac{1}{\rho}\nabla p + \nu\nabla^2 u = \frac{\partial u}{\partial t} + (u \cdot \nabla)u \tag{2.1}$$

$$\nabla \cdot u = 0 \tag{2.2}$$

which at low Re simplify to:

$$-\frac{1}{\rho}\nabla p + \nu\nabla^2 u = 0 \tag{2.3}$$

$$\nabla \cdot u = 0 \tag{2.4}$$

The zero-divergence condition remains the same as both flows are considered to be incompressible. Inertial effects are negligible, and all motion is quasi-static. There can be assumed to be no body forces.

2.2 Reversibility

In the Stokes Limit, flow exhibits reversibility. This phenomenon implies:

- effects of the reverse of a certain motion can be analyzed by reversing the time
- machines that exhibit time-reversible motion undergo no net translation.

Childress [4] proves that an organism moving with time-reversible motion cannot swim. If a neutrally buoyant organism swims through a fluid at an average velocity of U and its boundary is described by the function $S(t)$, the velocity of the organism can be broken into the sum of three components:

$$u = U + u_1 + u_2$$

The two perturbations u_1 and u_2 satisfy the no-slip condition of the surface and decay to zero at infinity.

$$u_1(S) = -U, u_1(\text{inf}) = 0$$

$$u_2(S) = \dot{r}_s, u_2(\text{inf}) = 0$$

where $\dot{r}_s$ is the velocity of the organism's boundary. Then u_2 is the velocity field associated with the movement of the boundary while u_1 is there to satisfy the field resulting from the a fixed boundary moving at U.

The net force on the organism is similarly decomposed into two components, the sum of which should be zero in free swimming

$$F_1 + F_2 = 0$$

where F_1, and F_2 are the forces associated with the different velocity fields U, u_1 and u_2. u_1 can be written as $u_1 = B\dot{U}$ where the tensor field B depends only on the organism boundary $S(t)$

The work done by the organism is described by the equation

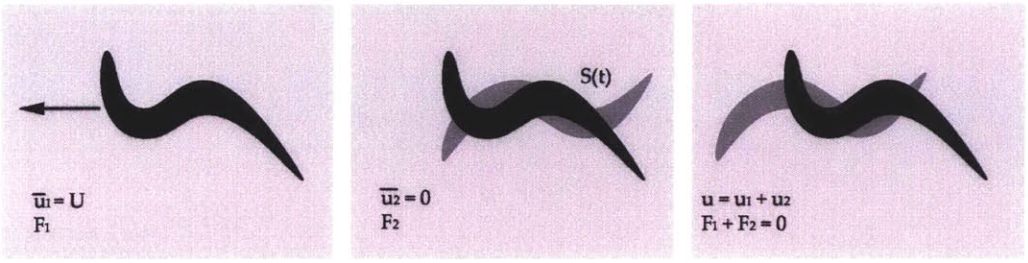

Figure 2-1: Motion of an organism at low Reynolds number. The net force can be seen as the sum of the force generated by the organism F_2 if it were held stationary while it strokes, and the force F_1 coming from dragging the rigid shape at whatever velocity u_1 required to cancel F_2.

$$F1\dot{U} + \Phi_1 = 0$$

where Φ_1 is the viscous dissipation associated with the motion u_1 of dragging the fixed shape through the fluid.

If a similar organism moves with the reverse motion (with respect to time), its boundary must follow $S^*(t) = S(-t)$. u_2 and F_2 are replaced with $u_2^* = -u_2$ and $F_2* = -F_2$. u_1 is satisfied for $u = -U$ on the boundary $S(-t)$ If the motion of the second organism is indistinguishable from that of the first, symmetry implies that $F_1^* = F_1$.

$$F_1^* + F_2^* = 0$$

$$F_1 + -F_2 = 0$$

which can only be satisfied when $F_2 = F_1 = 0$. The dissipation $\Phi_1 = 0$, implying zero net velocity. Thus an organism cannot swim if its motion is time-reversible.

2.3 Thin Films and Lubrication Theory

Flow between thin films is a subset of Stokes flow. Because the flow is confined to a space that is much thinner than its width (2-2), further simplifications can be made

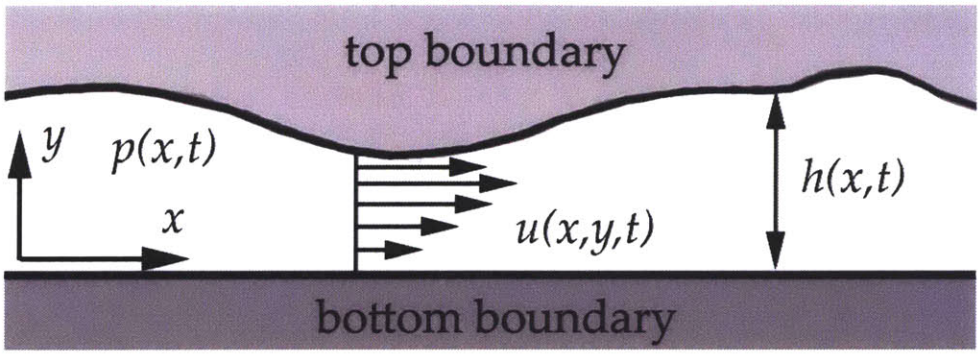

Figure 2-2: Lubrication flow. Velocity profiles are parabolic and pressure varies only in the x-direction.

to the governing Stokes equations, leaving the lubrication equation:

$$\frac{dp}{dx} = \mu \frac{d^2u}{dy^2} \tag{2.5}$$

which give the following implications:

- Pressure only varies in the x-direction
- x-velocities are assumed to be much greater than y-velocities
- inertial effects are negligible.
- velocity profiles are parabolic at all locations x in the film.

2.4 Non-Newtonian (Shear-Thinning and Finite Yield Stress) fluids

Snails and Robosnail 2 move using adhesive locomotion, requiring the use of a finite yield-stress liquid. The ability of the thin fluid layer to solidify and liquefy depending on strain rate allows snails to scale walls. Real snails have a continuous muscular foot while Robosnail 2 has a five-part discretized foot. Separation of the foot into the five parts allows for more precise actuation of the foot and a cleaner analysis of the motion.

We used Laponite as a substitute for snail mucus. Laponite is a suspension of clay particles in water, used as a thickening agent. In concentrations above 3 percent, it solidifies into a gel. Like snail mucus, Laponite exhibits finite yield stress, shear thinning, and aging properties. It was found that both snail mucus and Laponite samples behave as Herschel-Bulkley fluids, which have a stress profile that closely follows equations of the form:

$$\tau = \tau_0 + c\dot{\gamma}^k \tag{2.6}$$

where τ is the stress, τ_0 is the yield stress, $\dot{\gamma}$ is the strain rate. The values of τ_0, c and k were found to be $\tau_{0(mucus)}$ = 50 Pa c_{mucus} = 50 Pa k_{mucus} = 0.5 and $\tau_{0(Laponite)}$= 40 Pa $c_{Laponite}$ = 100 $k_{Laponite}$ = -1.1. (Snail mucus data is from Denny [6]) It can be debated whether the high-concentration Laponite truly is a Herschel-Bulkley fluid due to its negative exponent k. This negative value would lead to a theoretical curve that goes to infinity near a strain-rate of zero. The true yield stress of the Laponite was found by experiment to be around $\tau_{0(Laponite)}$= 120 Pa

The stress-strain profiles of 8 percent Laponite and snail mucus are plotted in Figure 2-3. The effect of the difference in the power k is clearly shown - surprisingly, the shear stress of Laponite decreases at higher strain rates, a result that yields interesting effects relating to the motion of Robosnail 2.

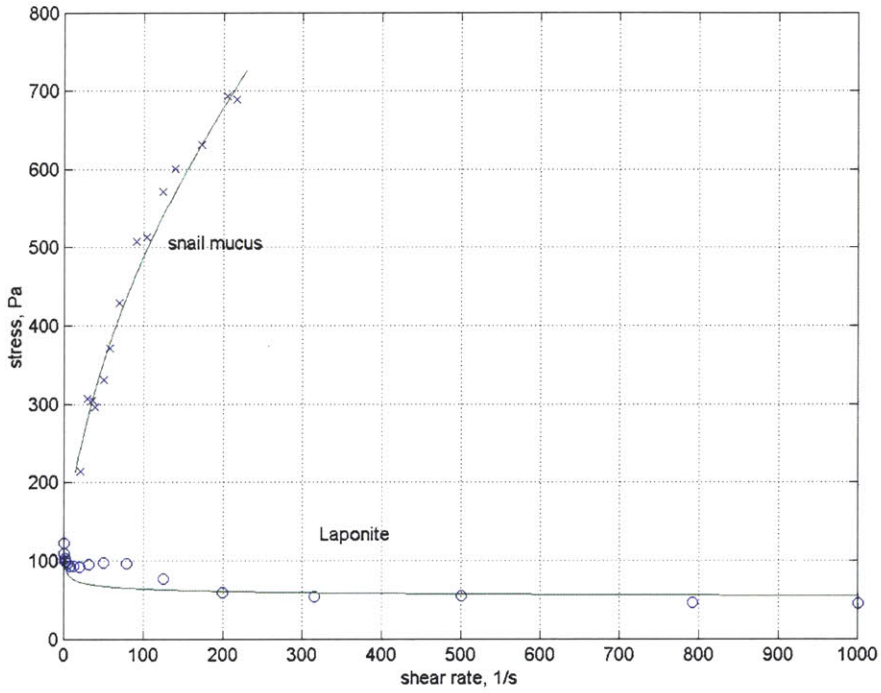

Figure 2-3: Stress vs strain rate curves of snail mucus and of Laponite. Concentration of Laponite is 8 percent by weight.

Chapter 3

The Three-Link Swimmer

3.1 Introduction

The concept of the three link swimmer was described by E.M. Purcell in his talk "Life at Low Reynolds Number" [11]

> There is a very funny thing about motion at low Reynolds number, which is the following. ...if (an) animal tries to swim by a reciprocal motion, it can't go anywhere. Fast or slow, it exactly retraces its trajectory and it's back where it started. ... The moral of this is that the scallop at low Reynolds number is no good. ...The simplest animal that can swim that way is an animal with two hinges. I don't know whether one exists ..."

Because of reversibility, a two-link swimmer would not be able to translate in the Stokes limit. Whatever displacement achieved by a single stroke would be canceled by the exact same displacement in the opposite direction, once the first stroke is reversed in the backstroke. Therefore, the a swimmer made of three links is the simplest swimmer consisting of rigid links hinged by reciprocating rotary joints. It can be argued that a body with a rotating flagella is simpler as it contains only one joint, however, the motion of the hinge connecting a flagella is not reciprocal. The fact that the motion of the three-link arms is oscillatory rather than steadily rotational allows for use of possibly simpler actuators than rotating motors.

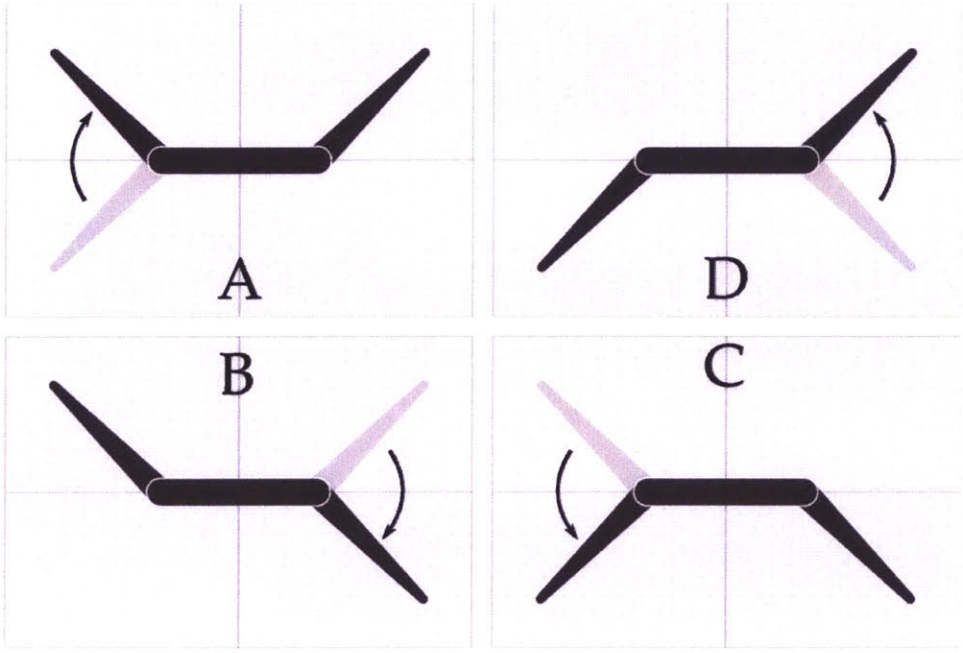

Figure 3-1: Motion sequence of three-link swimmer

3.2 Theory

The presence of three linkages allows the three-link swimmer to move in a non-reciprocal motion. The movements of the fins alternate: if the two ends of the swimmer are labeled P and Q: P rotates left, Q rotates left, P rotates right, Q rotates right and the cycle repeats. The net motion of the swimmer can be analyzed by looking at a single stroke. The three remaining strokes are either mirror images and/or time reversals of the first test stroke. Adding the translation resulting from the four strokes shows that though the sideways motion of the swimmer is oscillatory, the lengthwise motion is not.

Becker et al. [10] have made a theoretical model of the three-link swimmer using slender-body approach. Their model consists of three thin rigid filaments of small diameter rather than three rigid plates. It can be shown that there must be a difference between the drag of Low-Re flow hitting a filament section perpendicularly vs the drag of parallel flow- in order for the thin-body three-link swimmer to experience net translation.

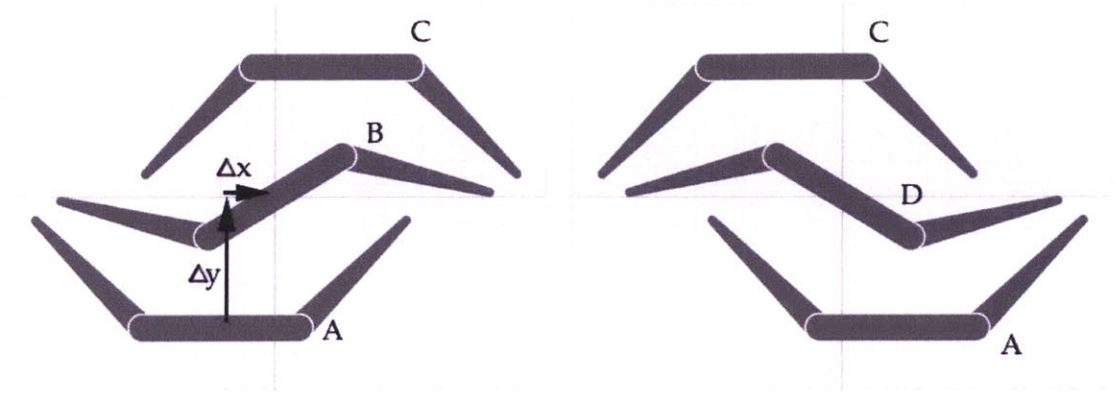

Figure 3-2: Analysis of the motion sequence of three-link swimmer. B-C is simply the time reversal of the 180 degree rotation of A-B, C-D is the 180 degree rotation of A-B, and D-A is the time reversal of the mirror image of A-B. The total distance traveled in one cycle is $4\Delta x$ Note: displacements are not drawn to scale.

Though the three-link swimmer prototype presented in this thesis is not composed of thin filaments, the results should be qualitatively similar.

3.3 Design

The swimmer consists of three main sections, the central body and two fins. It is powered by a coiled steel spring housed within the body. At the center of the coil spring is a one-way ratcheted rotatable hub that can be turned using a screwdriver. The outside end of the coil spring is attached to rotating cam. The outer face of the cam is composed of ten sections, alternatingly facing left and right by 45 degrees. The cam contacts either fin at on a line defined by a protruding ridge. As the spring unwinds, it rotates the cam, forcing the fins left and right in the proper sequence. The two ridges of either fin do not lie on the same plane as the axis of the cam; instead, they are situated off-center by half a cycle so that when one fin is being driven to one side, the other fin has not reached the actuation point. Otherwise, both fins would flip at the same time and the motion would be reciprocal. Since there are five sets of left-and-right sloped surfaces on the cam, each full revolution of the cam drives the swimmer through five cycles. The three-link swimmer operates submerged with its

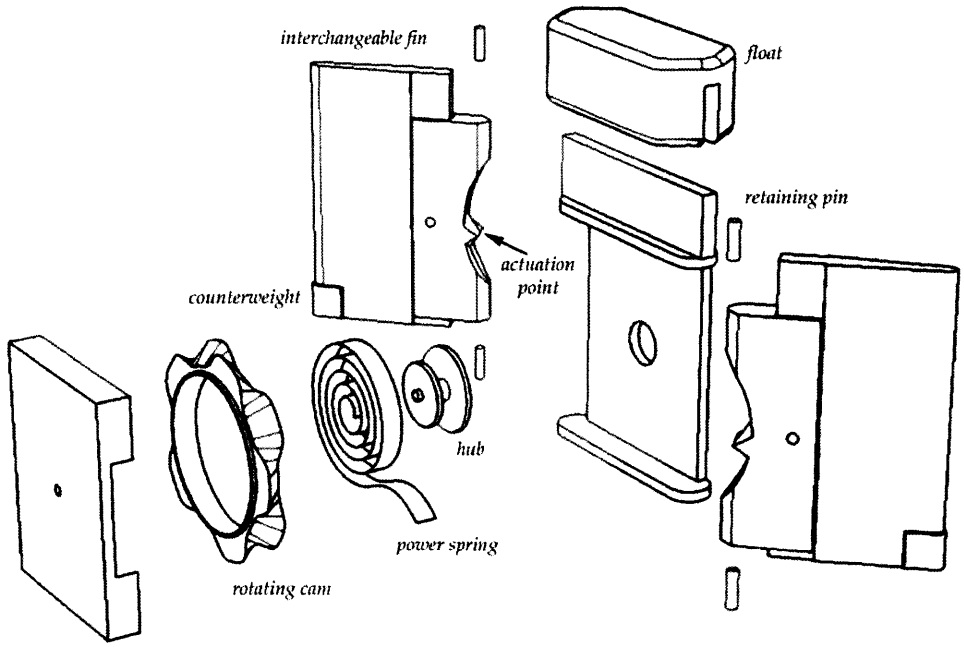

Figure 3-3: Exploded view of three-link swimmer

inner workings completely immersed in polydimethylsiloxane (PDMS, $\mu = 9.8$ Poise), which serves to lubricate the cam-body pivot and the cam-fin interface to prevent sticking, and to significantly slow the motion to ensure the swimmer operated in the Low-Re regime.

3.4 Results

The most noticeable component of motion experienced by the swimmer is side-to-side, but careful observation will reveal that the swimmer always has a preferred direction of motion, tending toward the side of leading arm. (The leading arm is the one that rotates to a certain side first, followed by the trailing arm.) This is the same direction of motion as for the planar swimmer predicted in theory and simulation by H. Stone et al. The theoretical swimmer modeled by Stone was composed of thin filaments while ours was composed of flat segments. Qualitatively, the results were similar as could be expected.

The center of the swimmer moves in a zigzag trajectory. Simple analysis of the

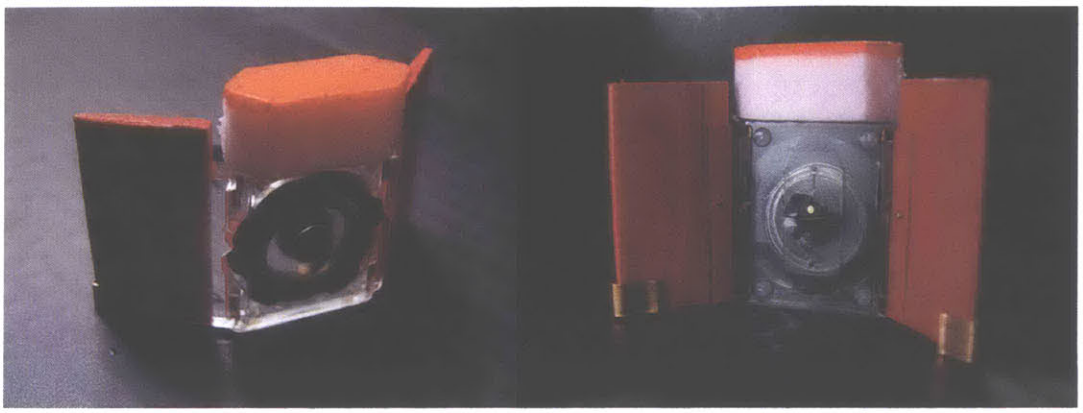

Figure 3-4: The three-link swimmer, front and back views, showing winding mechanism(center), float, and interchangeable fins

theory shows that motion in the y-direction is oscillatory while the motion in the x-direction is not. This is illustrated in Figure 3-2 (The displacement is greatly exaggerated in the figure; the true displacement of the swimmer per cycle is only a percent of the swimmers length at its greatest.)

The net translation per cycle is normalized to the total swimmer length l, which is the sum of the linkage lengths $l = 2a + b$ where a is the arm length and b is the body length. This way, it is known that at the limits $a/l = 0$ (no arms) and $a/l = 1/2$ (scallop case - reciprocal motion) there is no net translation, so the ends of the graph are fixed at zero. The data shows that there is a maximum translation per cycle around $a/l = 0.4$.

Addition of small, neutrally buoyant particles into the fluid allows visualization of the flow around the three-link swimmer (Figure 3-6). Lines drawn into the mixture in the form of a grid deform as the swimmer moves through the fluid. Several qualitative results can be drawn from the flow visualization. The deformation of the drawn grid lines demonstrates incompressibility: in areas where the vertical lines are stretched apart, horizontal lines are drawn closer together. Because of the no-slip boundary condition at the surface of the swimmer, fluid is dragged along as it swims. This is evidenced by the leading bulge of fluid and the fact that vertical lines remain attached to the swimmer. As the swimmer and the local fluid move in the forward direction, fluid is displaced backward, shown by the backward bulge of the vertical lines.

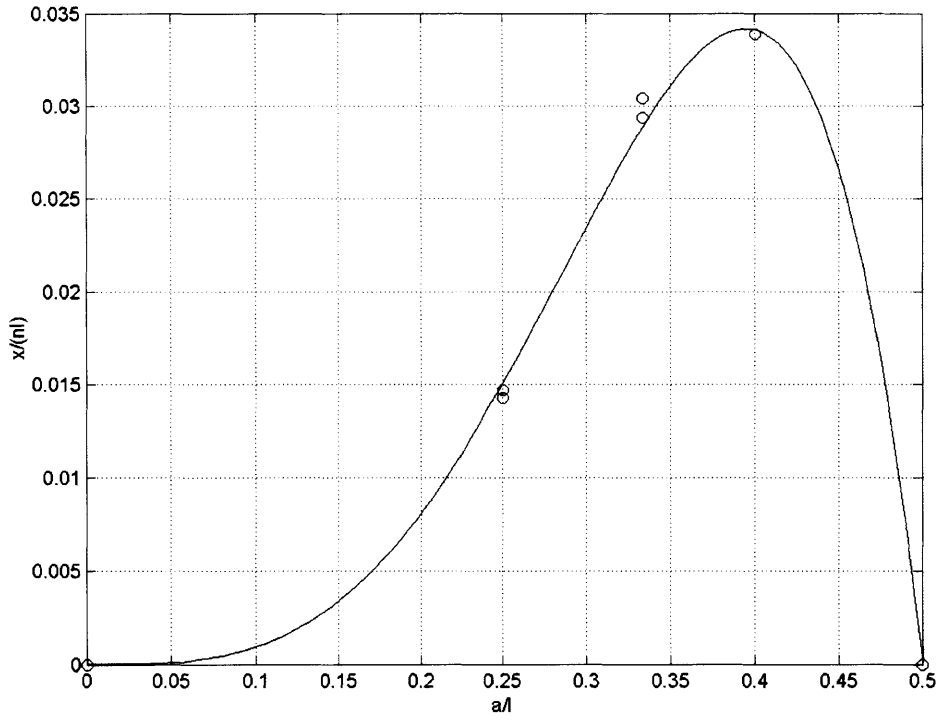

Figure 3-5: Net translation per cycle as a function of arm length, normalized to total body length (l = 2a + b). Note the zero points at a/l = 0 and a/l = 0.5 The curve $y = 1.95x^{3.3}(1 - 4x^2)$ is included merely as a likely interpolation and was not derived from any theory.

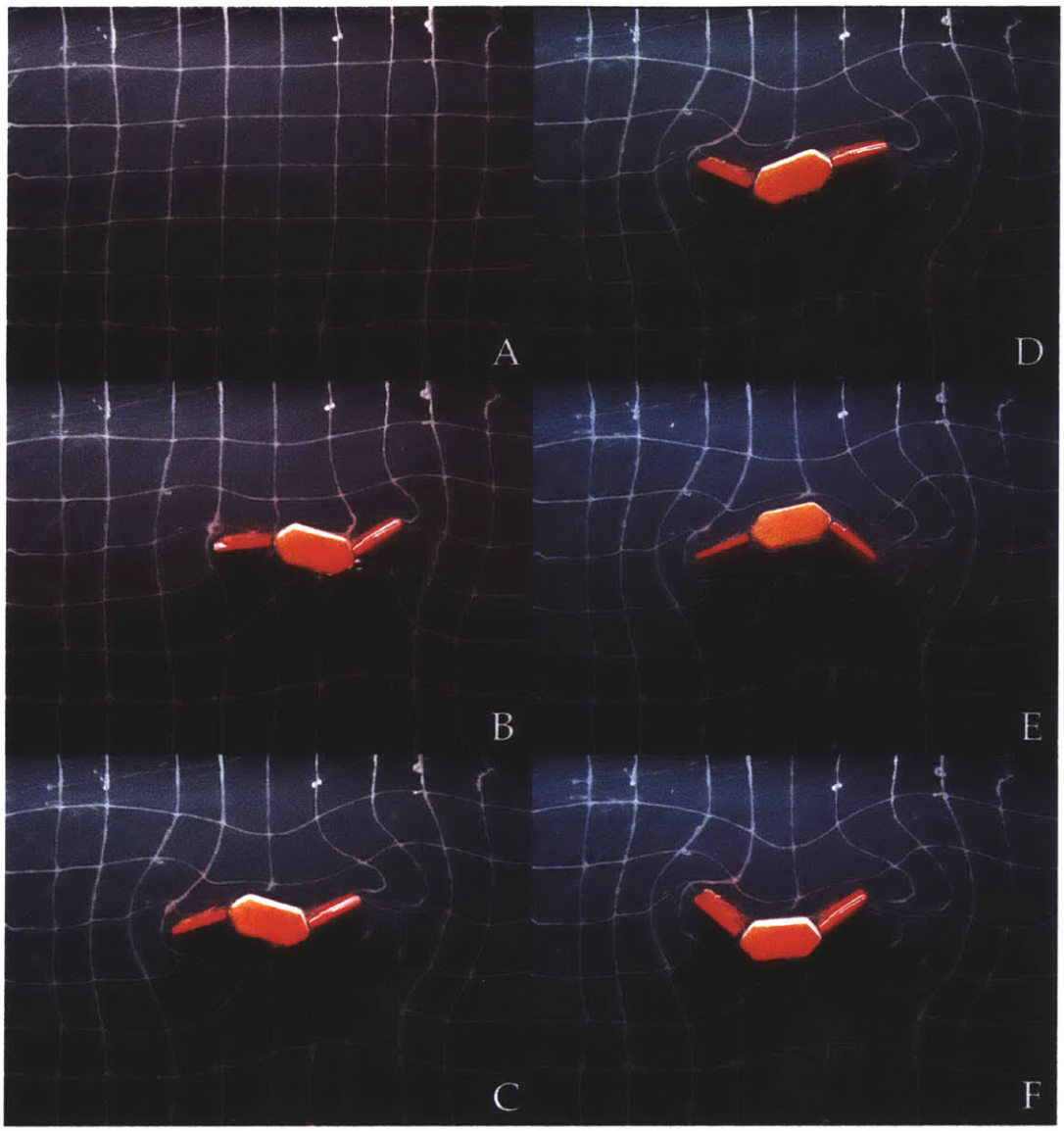

Figure 3-6: Flow visualization of the three-link swimmer in motion. (A) shows the undisturbed lines of particle-laden silicone oil laid into the clear oil. Because of the high viscosity of silicone oil, the lines remain undisturbed by small disturbances such as convection and vibrations throughout the duration of the experiment. About seven full stroking cycles are executed by the swimmer as it translates approximately 2 cm forward. The grid lines form a distinct hourglass shape in the vicinity of the swimmer.

Chapter 4

Robosnail 1 (Waving Sheet Lubrication Swimmer)

4.1 Introduction

The moving boundaries separated by a lubricating layer of viscous fluid can create high pressures as in the case of oil-filled bearings. In the case of the digestive tract of vertebrates, peristaltic motions create similar pressures to transport contents through the intestine [8]. In nature, several species of holothuroid (sea cucumber) are found to use peristalsis as a means of locomotion [12]. It is possible that aquatic snails may also generate lubrication pressures to aid locomotion. Periwinkles (*Littorina* sp.) and several aquatic snails are seen to generate backward propagating (retrograde) waves while in motion. Of the three land snails observed, all used forward (direct) waves in locomotion. It will be shown in the following sections that locomotion using lubrication pressures makes use of retrograde waves. The fact that aquatic snails use retrograde waves to move may be an indication that lubrication pressures play a significant role in their propulsion. It is possible that aquatic snails are able use the ambient water as a lubricating fluid, while land-dwelling species lack sufficient amounts water to move in this way.

A deformable, moving boundary creates lubrication pressures which act on the sloped boundary, resulting in a nonzero horizontal component of force, which can be

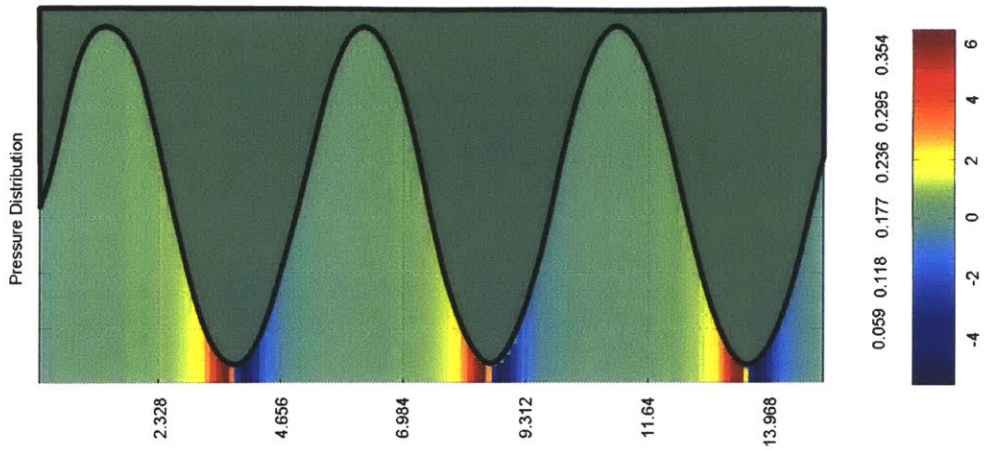

Figure 4-1: Pressure forces generated in fluid under a sinusoidal waving sheet. Pressure was calculated numerically by solving the lubrication equations for the periodic case of a sinusoidal waving sheet. There is a high-pressure zone immediately in front of the lowest point in the wave, where the fluid is being squeezed, and a low pressure zone immediately behind, where the fluid is being pulled apart.

used as a means of propulsion. One of the simplest forms of a steady, deforming surface is the sine wave. A sinusoidal traveling wave surface situated near a flat, solid boundary will generate high pressures to one side of the wave trough where the fluid is being squeezed, and low pressure on the other side of the wave, where the local volume is being expanded. This means of locomotion bears much similarity to the peristaltic pumping of fluids through flexible channels. The difference is that the force applied by the boundary is transmitted through the fluid to the substrate boundary, rather than being used to pump the fluid alone.

It was found that marine snails often exhibit retrograde waves that travel from head to tail, unlike land snails, which generally use direct waves, starting at the tail and end at the head. There is a possibility that marine snails and other aquatic creatures such as flatworms use backwards waving deformations of the body to generate thrust forces.

4.2 Theory

The fluid within the fluid layer then follows the lubrication equation:

$$\frac{dp}{dx} = \mu \frac{d^2u}{dy^2} \tag{4.1}$$

Pressure varies only in the x-direction

$$\frac{dp}{dx} = f(x)$$

Integration once with respect to y gives

$$\frac{du}{dy} = \frac{1}{\mu}\frac{dp}{dx}y + A$$

which shows that velocity profile is parabolic.

$$u = \frac{1}{2\mu}\frac{dp}{dx}y^2 + Ay + B$$

where A and B are constants, which can be solved for by considering the boundary conditions. Analysis of the flow is greatly simplified by considering a frame of reference in relation to the wave crests.

The velocities at the foot surface and the substrate are known:

$$u(h) = -v_w$$

$$u(0) = -v_w + v_s$$

where v_w is the wave velocity of the snail, defined in the frame of the snail and v_s is the snail velocity defined in the lab frame. The constants are solved from the boundary conditions:

$$B = u(0) = -v_w + v_s$$

$$u(h) = -v_w = \frac{1}{2\mu}\frac{dp}{dx}h^2 + Ah - v_w + v_s$$

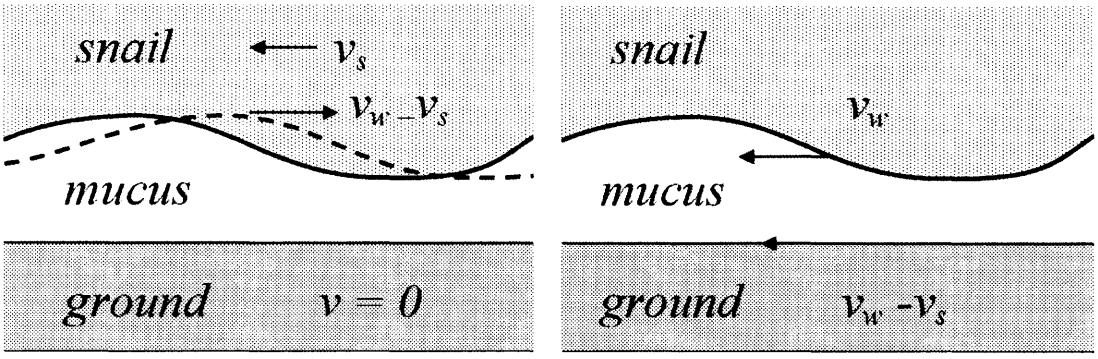

Figure 4-2: Left: Lab reference frame. Right: reference frame of wave crests. In the second frame of reference, the boundaries are fixed and the flow is steady.

$$0 = \frac{1}{2\mu}\frac{dp}{dx}h^2 + Ah + v_s$$

$$A = -\frac{1}{2\mu}\frac{dp}{dx}h - \frac{v_s}{h}$$

The velocity profile is then

$$u = \frac{1}{2\mu}\frac{dp}{dx}y^2 + (\frac{1}{2\mu}\frac{dp}{dx}h - \frac{v_s}{h})y - v_w + v_s$$

which simplifies to

$$u = \frac{1}{2\mu}\frac{dp}{dx}(y^2 - yh) + v_s(1 - \frac{y}{h})y - v_w \tag{4.2}$$

The height of the foot h is a function of time and distance along the foot. In a frame of reference following the wave crests, analysis of the flow is greatly simplified. h is now independent of t and only a function of x

$$h = h_0 + asin(x)$$

where h_0 is the average height, an unknown constant to be determined by force balance.

Volume flux Q:

$$Q = \int_0^h u dy = [\frac{\mu}{2}\frac{dp}{dx}(\frac{y^3}{3} - \frac{hy^2}{2}) + v_s(y - \frac{y^2}{2h}) - v_w y]|_0^h$$

$$Q = \frac{1}{12\mu}\frac{dp}{dx}h^3 + (\frac{v_s}{2} - v_w)h \tag{4.3}$$

Because the height of the waves becomes fixed, the flow is steady and as a result volume flux remains constant. Solving for the gradient of pressure,

$$\frac{dp}{dx} = \frac{12\mu Q}{h^3} + \mu(\frac{v_s}{2} - v_w)\frac{1}{h^2}$$

Integration along the x direction gives the expression for pressure.

$$p(x) = \int \frac{dp}{dx}dx + p_0$$

$$p(x) = \int (\frac{12\mu Q}{h^3} + \mu(\frac{v_s}{2} - v_w)\frac{1}{h^2})dx + p_0 L$$

$$p(x) = -12\mu Q \int \frac{1}{h^3}dx + 12\mu(\frac{v_s}{2} - v_w)\int \frac{1}{h^2}dx + p_0 L$$

If h and x are made non-dimensional, $h^* = h/a$ and $x* = x/L$

$$p(x) = \frac{12\mu L}{a^2}(\frac{v_s}{2} - v_w)\int \frac{1}{h^{*2}}dx - \frac{12\mu QL}{a^3}\int \frac{1}{h^{*3}}dx + p_0 L \tag{4.4}$$

Assuming periodic wave deformation and pressure, we solve for Q, the flow rate (henceforth we take h and x to be non-dimensional, dropping * from $h*$ and $x*$) The net pressure difference over a wavelength must be zero.

$$p(L) - p(0) = \int_0^L \frac{dp}{dx} = 0$$

$$0 = \frac{-12\mu QL}{a^3}\int_0^L \frac{1}{h^3}dx + \frac{12\mu L}{a^2}(\frac{v_s}{2} - v_w)\int_0^L \frac{1}{h^2}dx$$

The non-dimensional volume flux

$$q = \frac{Q}{a(\frac{v_s}{2} - v_w)} = \frac{\int_0^L \frac{1}{h^3} dx}{\int_0^L \frac{1}{h^2} dx}$$

pressure is then a function of h_0/a

$$p(x) = \frac{12\mu L}{a^2}(\frac{v_s}{2} - v_w)f_1 + p_0$$

where

$$f_1 = \int \frac{1}{h^{*2}} dx - q \int \frac{1}{h^{*3}} dx +$$

The horizontal force is the sum of the pressure force acting on the sloped sections of the foot and viscous shear forces along the line of motion.

$$F_x = F_{x,p} + F_{x,s} = 0$$

$$\int_0^L p \frac{dh}{dx} dx + \mu \int_0^L \frac{du}{dy}|_h dx = 0$$

keeping in mind that the constant p_0 does not effect the horizontal force on the snail because the integral $\int_0^L \frac{dp}{dx} dx = h(L) = h(0)$ goes to zero for any periodic $h(x)$. The shear rate at the foot boundary is found to be

$$\frac{du}{dy}|_h = \frac{1}{2\mu} \frac{dp}{dx} h + \frac{v_s}{h}$$

Substituting in the equations for pressure, $\frac{du}{dy}$, $\frac{dp}{dx}$ and for simplicity's sake defining the following functions

$$A = \int (\int_0^x \frac{1}{h^{*2}} dx - q \int_0^x \frac{1}{h^{*3}} dx) \frac{dh}{dx} dx \tag{4.5}$$

$$B = \int \frac{1}{h^*} - q \frac{1}{h^{*2}} dx \tag{4.6}$$

$$C = \int \frac{1}{h^*} dx \tag{4.7}$$

one finds that the ratio $\frac{v_s}{vw}$ is only a function of the normalized wave shape. In theory the shape can be any periodic function, and for future versions of Robosnail, can be optimized. However, owing to the simplicity of the actuation mechanism (a rotating helix), the foot boundary of Robosnail 1 follows a simple sinusoid, which in the lab reference frame is: $h = h_0 + acos(x - (v_w - v_s)t)$ In the wave reference frame, $h = h_0 + acos(x)$ When h is in non-dimensional form, A, B, and C are all functions of the the shape of the wave and independent of the other variables. When h is sinusoidal, A, B and C are only functions of h_{av}/a.

Solving for $\frac{v_s}{v_w}$ gives

$$\frac{v_s}{v_w} = \frac{12A - 6B}{-6A + 3B + C} \tag{4.8}$$

which is graphed in Figure 4-3 as a function of h_0/a

One sees that the horizontal speed with respect to the wave velocity is only a function of h/a. As the mean height approaches a, the amplitude of wave height, the snail velocity approaches 1.5 times the wave velocity. Vertical force:

$$F_y = \int p(x) dx$$

$$F_y = \int p(x) dx + p_0 L = mg \tag{4.9}$$

The vertical force depends on not only the integral of lubrication pressures, but also from the product $p_0 L$, p_0 being the constant of integration from dp/dx. In theory, p_0 can be arbitrary, depending on what point x on the sinusoid one chooses to integrate $\frac{dp}{dx}$. In practice it depends on the flow characteristics of the foot. More specifically, the end effects at the front and rear of the foot determine the pressure. If the Robosnail is higher in front than in back, there should be high pressure pushing up the snail, similar to Newton's sliding sheet lubrication problem. If the front is lower than the

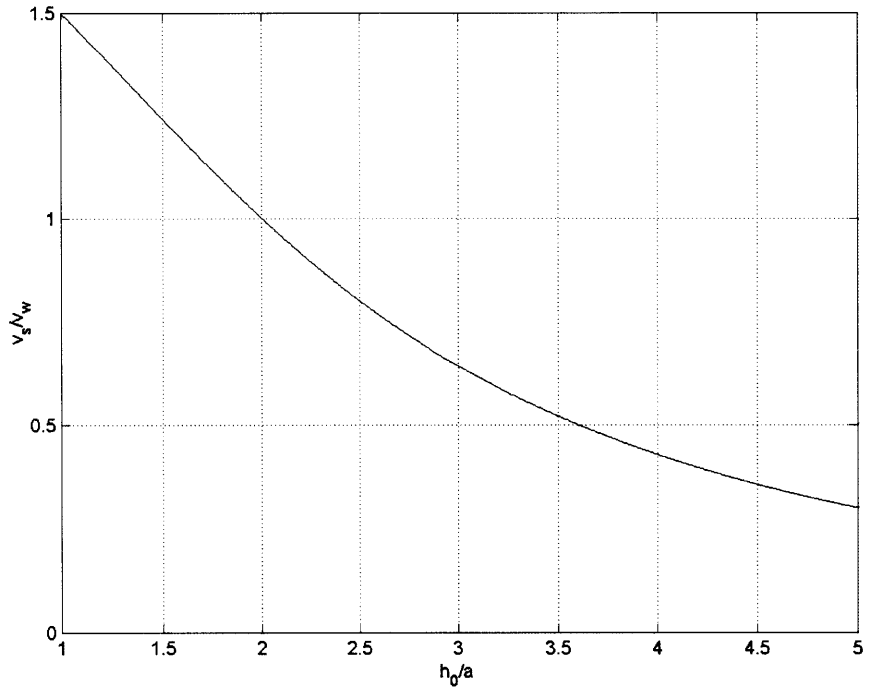

Figure 4-3: Robosnail ratio of wave speed to snail speed as a function of height for an infinitely long foot, two-dimensional case. Theoretically, the snail speed should be able to surpass the wave speed by 50 percent. In experiments, this does not occur and the snail speed is a fraction of the wave speed.

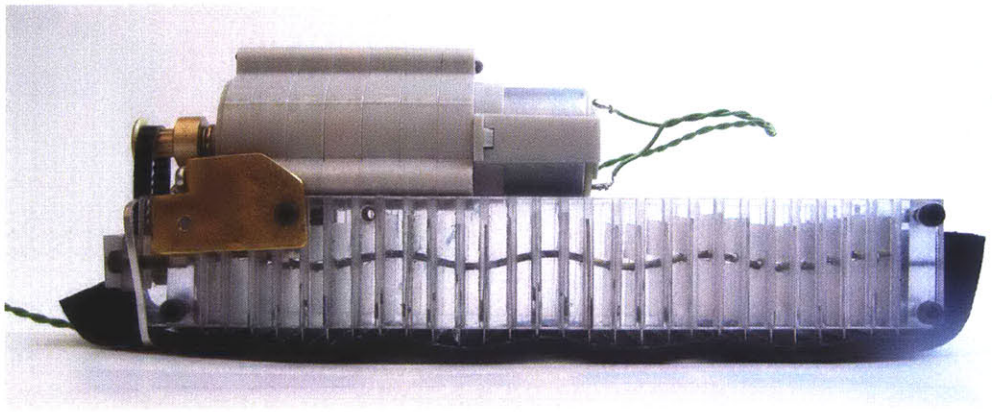

Figure 4-4: Robosnail 1, side view

back, there should be a suction instead.

4.3 Design

The Robosnail has a solid polycarbonate body. Its total weight is 1.67 N. Its foot is powered by an external DC power source, capable of supplying 1.5 , 3.0 and 4.5 volts. The motor is connected to a variable-speed gear box. A toothed pulley connects the gearbox to a shallow brass helix which passes through an array of aluminum sheets perforated with slots. Each of the sheets is constrained to vertical motion - they ride in equally spaced slots along the body. The bottom edges of the sheets are directly glued onto a flexible foam sheet. When the helix is spun by the motor and gearbox, it causes the plates to translate up and down inside their tracks in a moving sinusoidal wave (evident when seen from the side). The wave is transferred directly to the foam sheet.

The test track of Robosnail 1 (Figure 4-7) was constructed to be only slightly larger than the width of the snail to minimize the leakage of fluid past the open sides of the foot. A laser, fitted with a lens to emit a plane of light, was fixed at an angle of 45 degrees with respect to the bottom of the clear channel. The line of the laser hitting the foam sole, seen from the underside, reflects the height of the wave with respect to the bottom of the channel, and the profile of the film thickness becomes clearly visible from an underside view (Figure 4-6). The track was filled with 0.5 mm

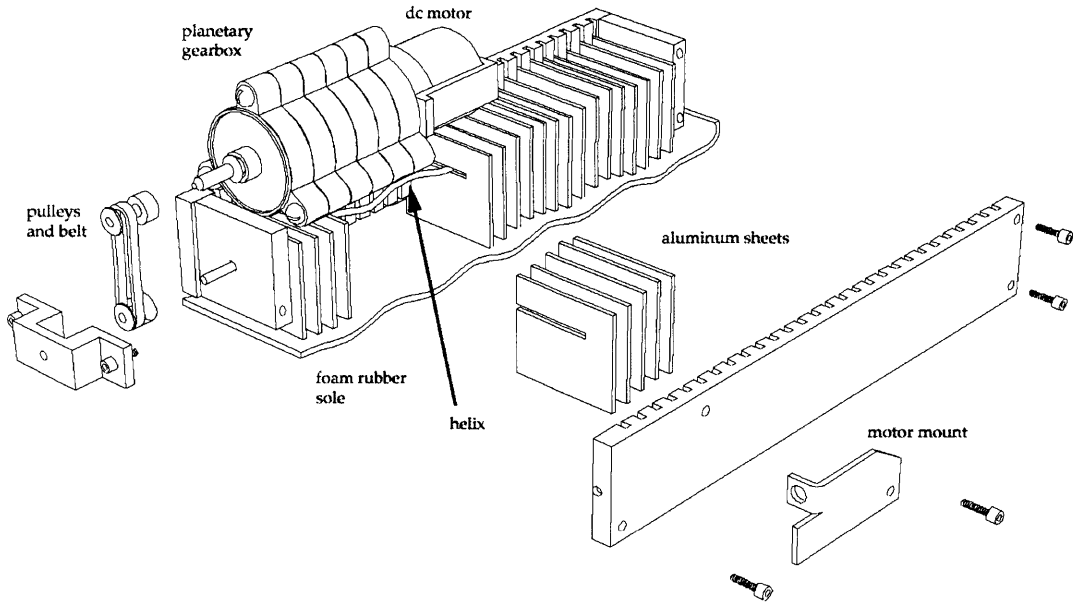

Figure 4-5: Robosnail 1 exploded view

thick layer of glycerol and the Robosnail was activated on top of the layer. After the motion reached steady state, measurements of wave speed, foot height (revealed by the laser), and snail speed were recorded by video.

4.4 Results

Robosnail 1 was tested using differing speeds on a layer of glycerol. Direction of motion was found to be opposite the direction of wave propagation. The speed of robosnail as a function of wave speed is plotted in Figure 4-8.

It was found experimentally that Robosnail 1 traveled at a height very close to the minimum $h/a \approx 1$ As predicted, the snail speed is approximately linear with respect to wave speed. However, the experimental velocity was found to be about 1/3 the expected value for the infinite two-dimensional case. The great discrepancy in speed is most likely due fluid leakage through the gap between the snail and the walls of the channel. Such leakage will greatly decrease the thrust from lubrication pressures while barely affecting the shear drag that is proportional to the speed of the snail.

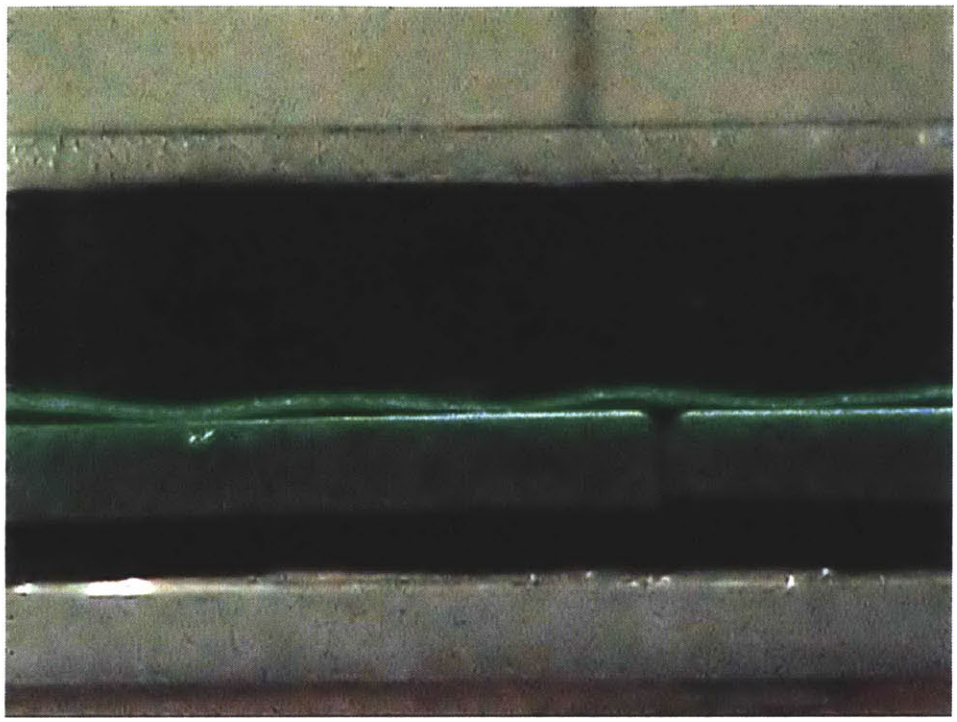

Figure 4-6: Robosnail 1 in motion, still from video. A sheet of laser light shining at an angle on the waving foot shows the foot height.

Whether or not marine snails use lubrication pressures as an aid to locomotion remains unknown. We have attempted to measure variations in the film thickness of moving periwinkles (*Littorina* sp.) using an angled laser setup similar to the Robosnail 1 experiment. Because the dimensions of the largest periwinkle foot are on the order of 1 cm, and owing to the diffusion of light through the translucent snail foot, the resolution of the angled laser technique was not fine enough to reveal any height variation.

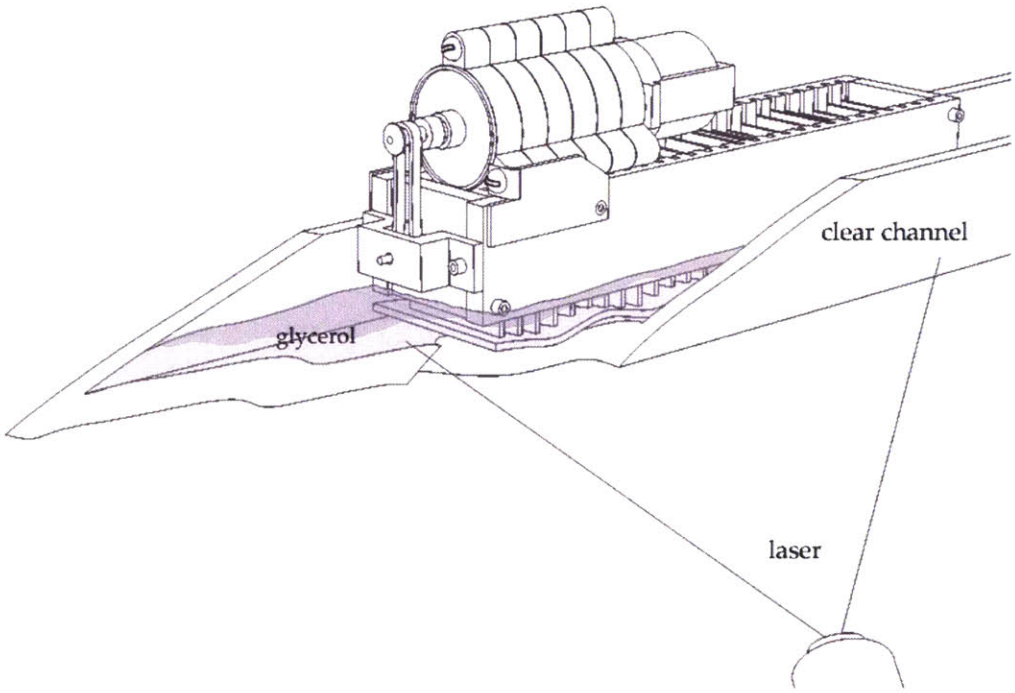

Figure 4-7: Robosnail 1 setup

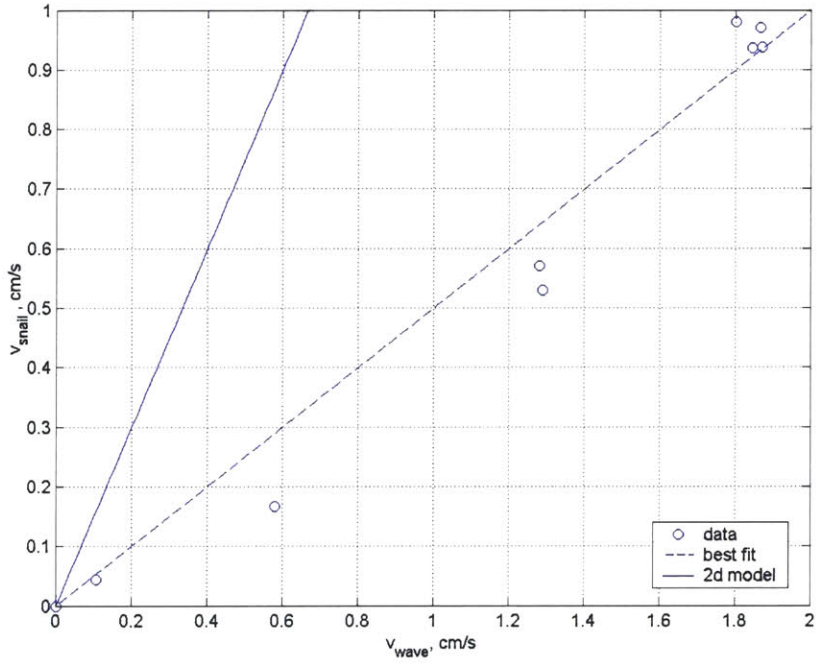

Figure 4-8: Robosnail 1 speed as a function of wave speed. Fluid: glycerol

Chapter 5

Robosnail 2 (Extensional Sheet Lubrication Swimmer)

5.1 Introduction

The second Robosnail relies on a mode of locomotion also used by land snails. The adhesive locomotion of a the banana slug *Ariolimax columbianus* (slugs are a subset of snails) was analyzed by M.W. Denny [7]. Land snail locomotion, though slow and messy, is worth studying for its versatility. Snails are observed to walk up walls, under ceilings, and along thin plant stalks with relative ease.

Snails move over a thin layer of mucus secreted onto the substrate by pores on the foot. The physical properties of the the mucus are important for the snail's ability to adhere to any surface and to move without lifting its foot. A certain pattern of muscular foot deformations allows the snail to effect an average forward velocity while the majority of the foot is glued down by the mucus layer.

Robosnail 2 has a sole of foam rubber sheet, much like Robosnail 1, but is only connected to five actuators. Instead of translating up and down, the actuators are restrained to move forward and back in the plane of the foot, extending and retracting the sections of the foot. In essence, it moves like a snail with discrete motion of segments instead of continuous motion, and only one wave on the foot at any one time. The basic phenomenon is the same, most of the foot remains attached to the

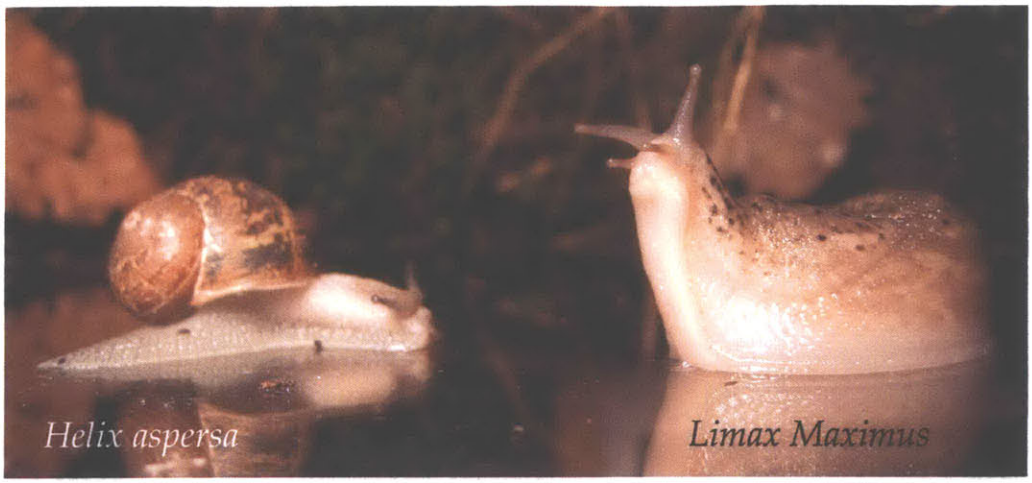

Figure 5-1: *Helix aspersa* and *Limax maximus*, two species studied in lab

floor while the net translation is effected by the motion of a small fraction of the foot.

5.2 Theory

Snail motion has been looked into in great detail by M.W. Denny [5], who made close observations of the moving foot of the banana slug, *Ariolimax columbianus*, a suitable species for study because of its large size. Our studies involved the locally obtainable giant leopard slug, *Limax maximus* and garden snail *Helix aspersa.* We found qualitatively similar results due to the similarity of size, morphology and locomotion style of the three species.

Figure 5-2 is a video still of a moving leopard slug as seen from below. Viewed from the underside of a transparent platform, a moving snail is seen to form a train of lateral stripes appearing at the tail, moving along the body, and leaving off at the head. (In many aquatic species the bands appear at the head and move toward the tail). Close observation shows that the bands are alternatingly wide and thin. The thin bands, known as waves, are in motion with respect to the substrate and in compression, while the areas of the foot within the wider bands, known as interwaves, are stationary with respect to the substrate. On either side of the central section is the rim, which is not observed to deform significantly during locomotion.

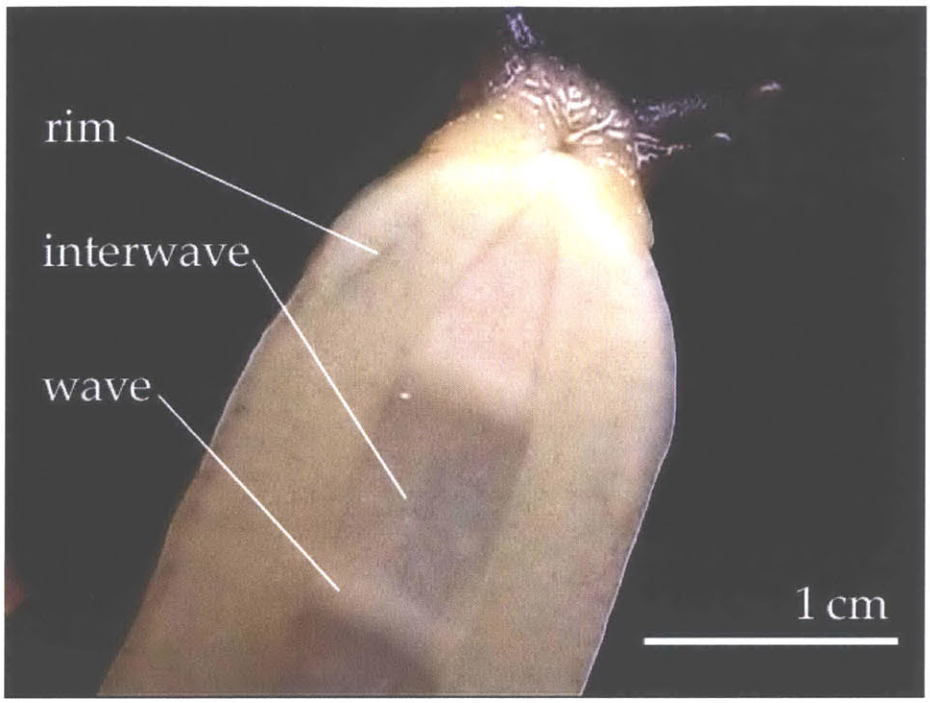

Figure 5-2: Foot of leopard slug *Limax maximus* in motion seen from below through a glass plate.

Denny was able to gain much insight into the details of the moving foot by quick freezing and sectioning of slugs which were in motion. He measured the thickness layer to be 10-20 μm and found that the compression ratio (defined as ratio of the relaxed distance to the contracted distance between cells) of the wave to be an average of 1.69. For a typical banana slug, Denny found between 13 and 17 waves generated during motion. The points of the central section where the waves and interwaves pass were found to spend an equal amount of time in and out of a wave. The point speed on an interwave is zero with respect to the ground. The velocity of a point on the snail's foot must average out to V, the average snail velocity. It was found by Denny in experiments using *Ariolimax columbianus* that a given point on the foot spends half of the total time inside a wave, therefore the velocity of a point inside a wave must be 2 V. The wave itself moves at a rate of 3.3 V, a faster speed than the point speed. Figure 5-3 plots the distance of a point on the foot of *Limax maximus* in motion. In the case of*Limax maximus*, the points spend a smaller fraction of time within a wave, resulting in a wave point speed of about 3.4 V and a wave speed of

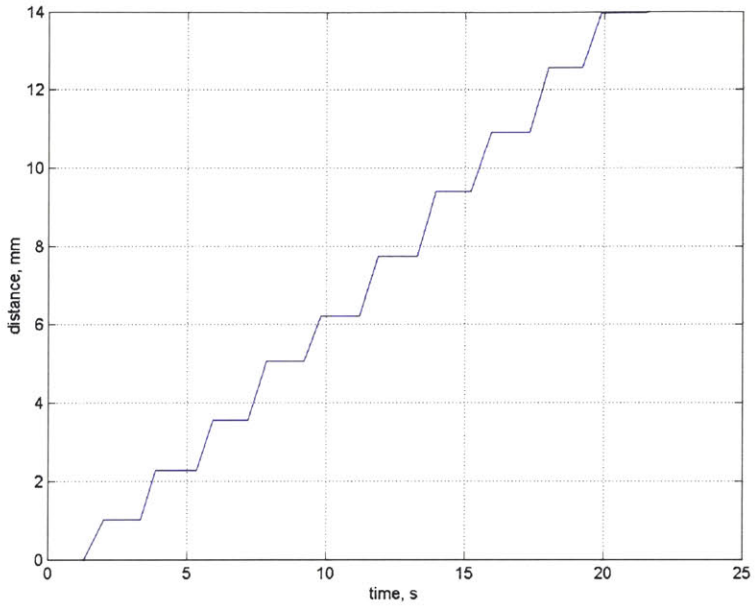

Figure 5-3: Distance plot of a point on the foot of a leopard slug *Limax maximus* in motion. The intervals where distance is constant indicates the times when the point resides in an interwave.

$8.1V$, both faster than the banana slug. Because the rim moves steadily and does not deform appreciably, it moves at the average speed V of the snail. The combined viscous forces of the shearing mucus underneath the moving rim and waves must be balanced by the elastic force of the stationary interwaves.

It was shown that the parameters of foot area, maximum slug size, mucus layer thickness, and wave speed are determined by the physical properties of mucus. The important properties of gastropod mucus that aid in snail locomotion are finite yield stress, shear thinning, and heal time. The heal time is the amount of time that a sample of mucus takes to re-solidify after shearing into liquid form. It limits the maximum speed of a snail by limiting the number of waves that can pass over any point in a given amount of time. If a second wave were to pass over a given area in too short a time to allow the mucus to heal, the snail would experience back-slip.

Robosnail 2 operates like real land snails. The bottom 'foot' of the snail is mostly adhered to the substrate while a traveling wave of compression (or elongation in the

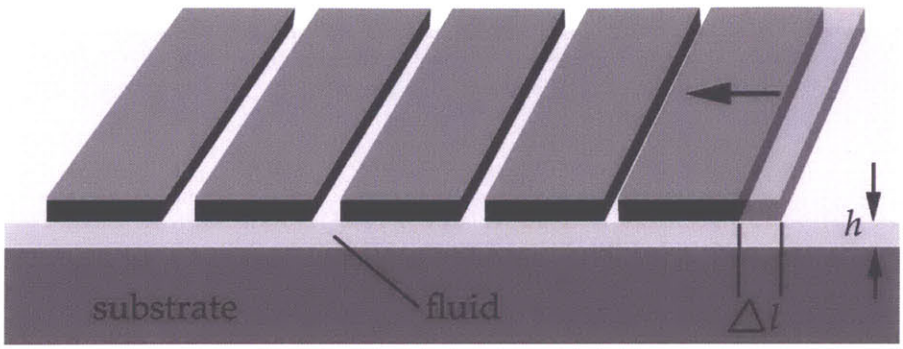

Figure 5-4: Robosnail 2 moving over a fluid. Fluid layer height is h. A foot segment shifts by a distance of Δl every T seconds.

case of marine snails) causes a small net translation as it propagates from one end of the foot to the other. The difference between locomotion of Robosnail 2 and real snails is that the foot of Robosnail 2 is made of five discrete, sliding sections, while real snails have a continuous foot of muscle. Each of the five foot sections of Robosnail 2 move in sequence 1, 2, 3, 4, and 5 forward a small fixed amount in relation to the body, after which they all return to their original positions.

Instead of mucus as a lubricating layer, Laponite was used. Laponite is a suspension of layered magnesium silicate particles in water [1]. It is used in the cosmetics industry as a thickening agent. Laponite was chosen as the Robosnail 2 lubricating fluid for its pronounced shear-thinning effects and its availability. Though the mechanical properties of Laponite and snail mucus are quantitatively different, both exhibit the similar non-Newtonian properties that allow for adhesive locomotion.

The lubricating fluid must be non-Newtonian for there to be a net translation. To prove this, we will first consider the case of a Robosnail 2 moving over a viscous Newtonian fluid in the lubrication limit (see Figure 5-4).

In order to simplify the analysis, we will treat the sheet as a perfectly flat plane separated from the substrate by a fluid layer of thickness h, and we will assume that instead of contracting, the foot is made of sliding segments. We will analyze the a foot that is comprised of n segments where only one segment is moving (with respect

to the rest) at all points in time. T is the time it takes for the deformation to reach from the back to the front. The amount of translation of each foot will be Δl For the Robosnail 2 prototype used in the following experiments, n= 5, T = 5 s, and Δl = 1 mm.

If we assume that the section of the foot not contracting does not slip, then the foot moves Δl every T seconds and the snail travels at a speed of $\frac{\Delta l}{T}$. Logically, there should be a certain amount of slip velocity, v_s between the $(n-1)/n$ sections of the foot and the substrate. As this is in the Low Re Lubrication limit, inertia can be neglected and the forces in concern are the viscous shear forces under the foot. We can treat the area under each foot section as Couette flow, where the shear rate is simply the difference of top and bottom velocities divided by the height, and the shear stress (since the flow is Newtonian) is viscosity by shear rate.

There are n foot sections. The moving foot section only moves during $1/n$ the time. Since the average velocity is $\frac{\Delta l}{T}$, the instantaneous velocity of the moving section is $n\frac{\Delta l}{T}$. The force balance between the contracting foot section and the rest of the foot is

$$F = -\mu v_s A/h + \mu n \frac{\Delta l}{T} A_2/h = 0$$

where A_2 is the area of the moving section while A is the full area of the foot. μ and h drop out from the equation leaving

$$-v_s A + n\frac{\Delta l}{T} A_2 = 0$$

$$v_s = \frac{\Delta l}{T}\frac{A_2}{A}$$

$$\frac{A_2}{A} = \frac{1}{n}$$

The net velocity is the contraction rate minus the slip velocity

$$v = \frac{\Delta l}{T} - v_s$$

$$v = \frac{\Delta l}{T} - n\frac{\Delta l}{T}\frac{A_2}{A}$$

$$v = \frac{\Delta l}{T}(1 - n\frac{1}{n}) = 0$$

Thus Robosnail 2 should not be able to move on a layer of Newtonian fluid.

Equation for motion using finite yield stress fluid: As long as the shear stress sustained by the non-moving portion of the foot is less than the yield stress of the Laponite layer, there will be no slip at the interwave and the translational velocity is $\frac{\Delta l}{T}$. The force balanced by the viscous shear of the moving part is equal to the force sustained by the stationary parts of the foot.

$$\mu A_1 v/h < A_2 \tau_{yield}$$

When the speed of the moving foot section is small, one can approximate the stress underneath the shearing Laponite by $\tau_{yield} = 100$ Pa and the force on the moving part of the foot to be $A_2\tau_{yield}$

The theory of motion for non-Newtonian fluid motion is not as simple. Rotating-vane rheometry of Laponite suspensions reveal that Laponite under stress undergoes localized shear [13] [3]. Likewise, yielding of the Laponite solution beneath the foot is not uniform. Experiments show that when Robosnail is activated on a layer of Laponite of a given thickness, the layer of liquefied Laponite is not the full thickness of Laponite, but only a thin layer bordering the foot. This effect arises because of the shear-thinning properties of Laponite. At shear strain rates higher than 200/s, the shear stress is only about half the yield stress of solidified Laponite solution.

The Laponite suspension behaves somewhat like a Herschel-Bulkley fluid, where the shear stress closely follows an offset power function :

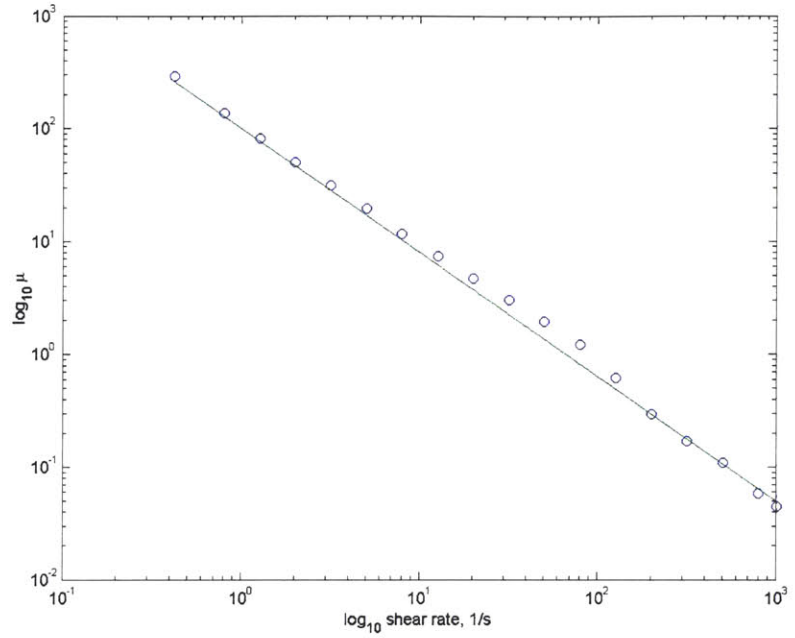

Figure 5-5: Laponite viscosity vs. shear strain

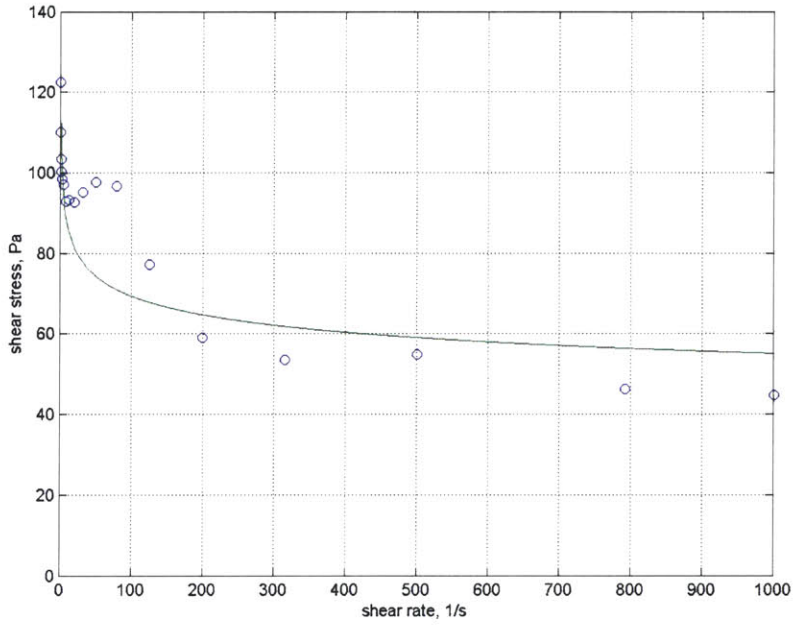

Figure 5-6: Laponite shear stress vs. shear strain.

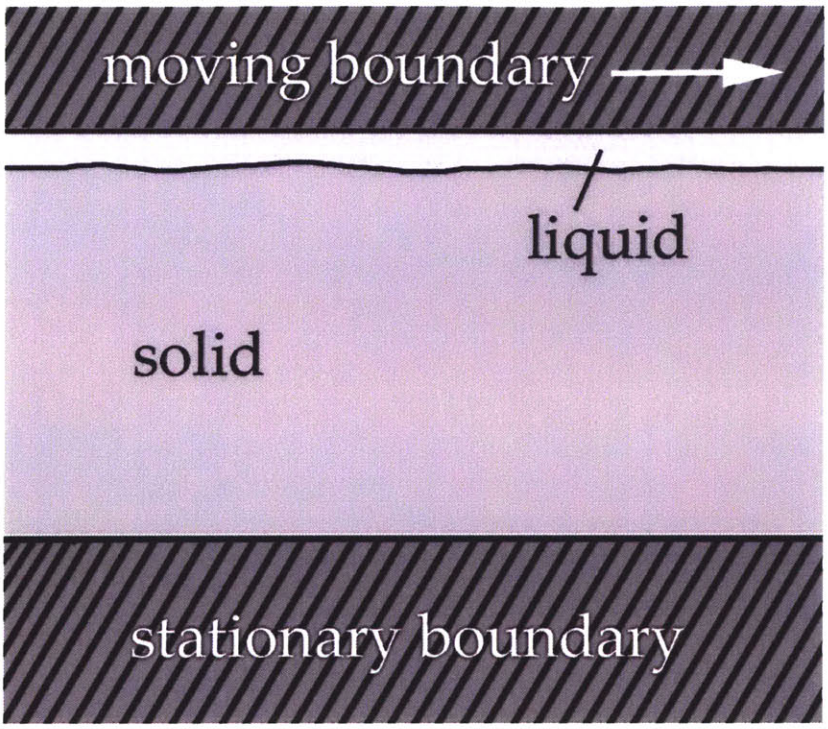

Figure 5-7: Laponite in shear. Not all of the Laponite thickness was observed to liquefy uniformly under applied shear stress higher than the yield stress; Most of the sample remains solid except for a thin layer of locally-yielding fluid.

$$\tau = b + c\dot{\gamma}^k \tag{5.1}$$

where $a_{Laponite}$= 40, $c_{Laponite}$ = 60 $k_{Laponite}$ = -.2, derived from rheometry. At zero strain rate, the model does not apply as it would predict a shear stress tending toward infinity. Instead, the experimental shear stress is observed to approach a value of about 100 Pa.

The thickness of the shear layer should reach an optimum where the total dissipation is minimized. In an infinitely wide layer of Laponite held between two sliding flat surfaces, there should form a division of two layers, one liquid layer over a solid layer. From a steady force balance, the stress τ is the same at any height within the sample. The Laponite within the solid layer follows the relation $\tau < \tau_{yield}$ while the fluid above the layer undergoes the same shear stress $\tau = \mu\frac{V}{h}$ where h is some height to be determined.

After yielding initially at τ_{yield}, stress within the Laponite layer can decrease to half the value if the strain rate is sufficiently high (in the range of 200 $1/s$ and higher). The fact that the stress throughout the layer is only a fraction of the yield stress allows most of the Laponite to remain solid while a small layer undergoes yield. Since the velocity of the top plate V, is fixed, the strain rate is V/h_{yield} and varies with h_{yield}, the height of liquid that forms from the shearing action. In the higher strain rates, τ varies little with strain rate and and V is fixed, therefore the viscous dissipation, τV is roughly constant. The optimal height of yielding fluid is the height which satisfies the requirement of minimum τ. In the case of Laponite, the value of τ reaches a steady value of about 50 Pa in the higher ranges, and the optimal strain rate is always 200 or higher. In the case of Robosnail, the characteristic velocities are on the order of 1 cm/s or less, and with the relation

$$V/h_{yield} = \dot{\gamma} < 200s^{-1}$$

gives h_{yield} of 0.05 mm or less. In experiments, the Laponite layer remained visibly intact despite the shearing action of the sheets, confirming that the shear layer is very thin relative to the total thickness of Laponite used (1.5 mm) It is worth noting that snail mucus, because its stress increases continually with higher strain rates unlike Laponite, does not shear in a thin layer like the Laponite suspensions. Snail mucus should instead undergo a more uniform deformation throughout a given sample. The effects of this difference of response to shear deserves more attention.

The fact that only a small layer of Laponite is necessary for effective motion of Robosnail makes Laponite and appealing compound for the adhesive locomotion of Robosnail type robots.

5.3 Design

Robosnail 2 was designed to take advantage of the vertical wall-climbing ability of adhesive locomotion using a shear-thinning fluid. Since the yield stress of Laponite is only about 100 Pa, we needed to be as light as possible. Instead of motors, Robosnail

2 is actuated using five 10 cm lengths of Nitinol shape memory alloy wire. The particular form of Nitinol used for Robosnail 2 is drawn into a wire that contracts 5 percent when heated. The Nitinol is well suited as an actuation mechanism because of its high force-to-weight ratio.

Nitinol is an alloy composed of Nickel and Titanium [9], exhibiting transition from martensite to austenite above the critical temperature of 70 degrees C. While it is in the cooled, martensitic phase, the Nitinol wire can be plastically deformed up to 8 percent. Heating the wire (using electricity, for example) will return it to its undeformed shape. The wire can act as a linear actuator when it is formed in such a way that the annealed shape is shorter than the deformed shape. It can be then freely stretched up to 8 percent in its cold state. The wire contracts when heated, but cooling the wire does will not extend the wire. A small force is necessary to return it to the stretched state.

The five Nitinol wires are attached to nylon cords wrapped 180 degrees around a pulley and tied to five sheets of polycarbonate. Each of the sheets is attached to a pair of guides that allow only fore-aft translation. A leaf spring held by the main body returns each of the sheets to its original position when there is no other force. The springs act apply the restoring forces necessary to return the wires to their outstretched positions.

The wires are crimped in loops at the ends, one end is tied to the cords controlling the foot, and the other end of each wire is looped around adjustable brass fasteners to allow proper tightening of the wire and cords. It was important for the wires to be at the right tightness that the springs succeed in re-stretching the wires, but not too tight such that the force applied during contraction is not enough to overcome the force of the spring. The tightness adjustment is achieved by turning the screws through which the wire mounts are threaded.

Yield stress of solidified aged, high-concentration Laponite was measured to be 390 N/m^2. This value is significantly higher than what was found from the rotating cone rheometry (120 N/m^2) because the latter sample was not allowed to age. The high value was used for estimates of actuator force requirement while the low value

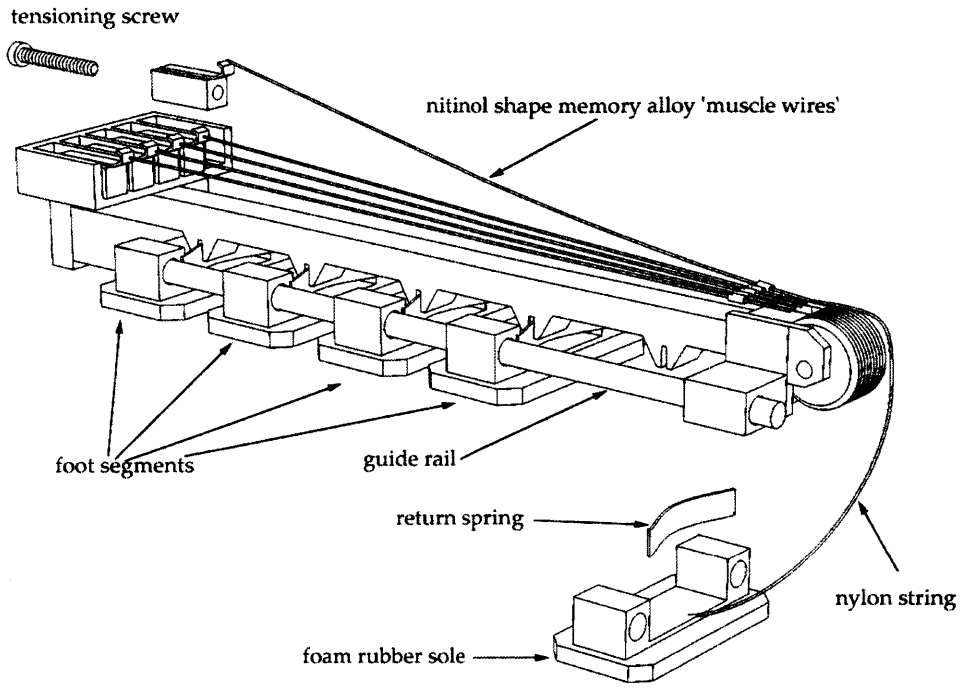

Figure 5-8: Robosnail 2 exploded view. The lead wires have been omitted for clarity.

was used for calculations of minimum required area to support the Robosnail. The area of the foot was designed such that the product of the area of $n-1$ feet segments by the yield stress of the Laponite to be used exceeded the weight of Robosnail by a safe margin. The finished robot weighted 0.31 N, while

$$(n-1)A_{seg}\tau_{yield} = 4 * 6.9cm^2 * 120Pa = 0.33N > mg$$

where A_{seg} is the area of a foot segment. This is a low estimate because the 120 Pa value for yield stress is the minimum for un-aged Laponite. This condition needed to be satisfied for the Robosnail to climb walls and ceilings. The measured yield stress of the Laponite mixture also aided in the choice of muscle wire size for actuation of the individual foot segments.

The five polycarbonate sheets are lined at the bottom with a neoprene foam rubber sheet, to comply more readily with irregularities in the substrate and Laponite layer. Voltage is applied to the Nitinol wires in the following sequence: 1, 1 2, 1 2 3, 1 2

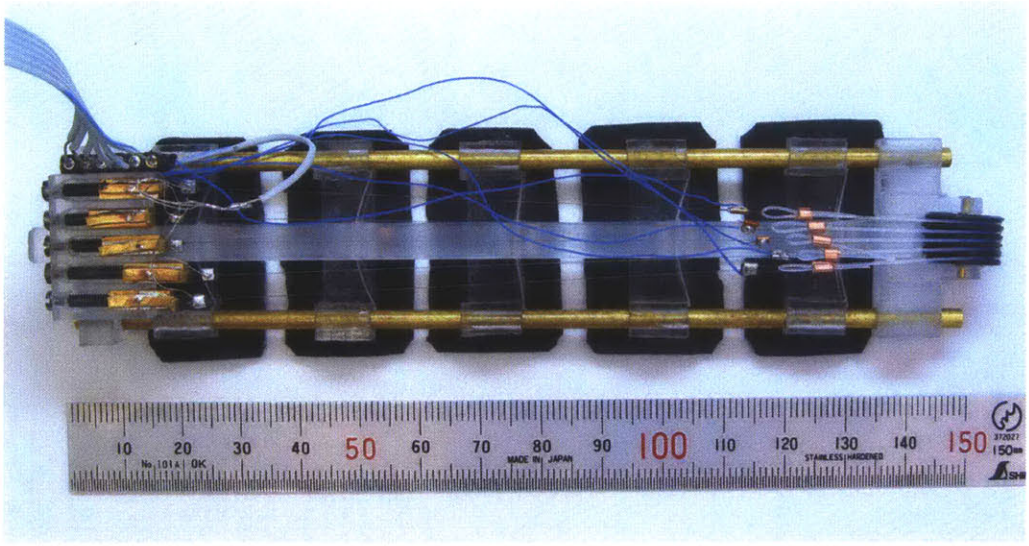

Figure 5-9: Robosnail 2 top view, showing muscle wire actuators.

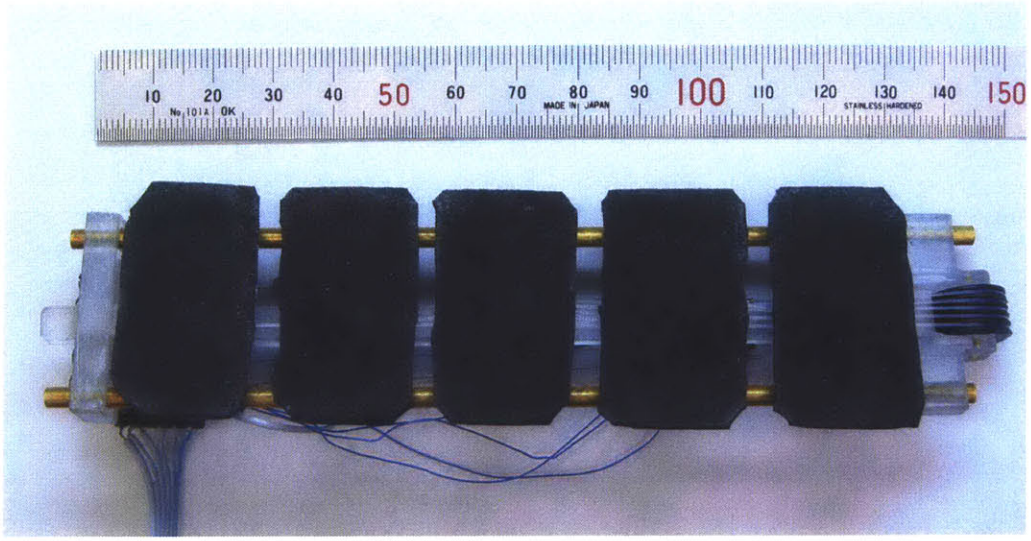

Figure 5-10: Robosnail 2 bottom view, showing neoprene foam rubber foot segments.

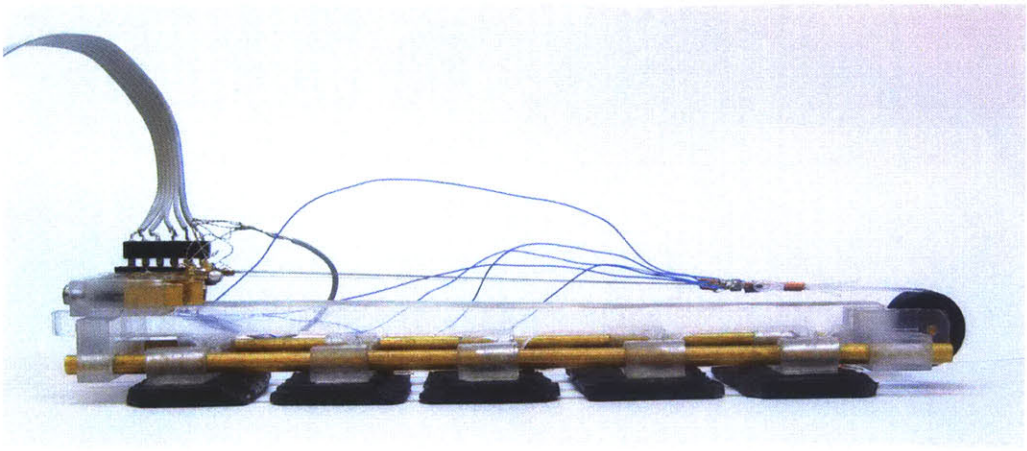

Figure 5-11: Robosnail 2 side view

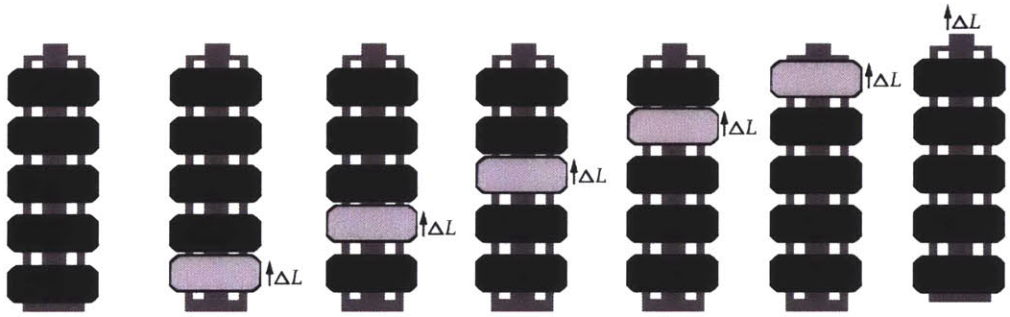

Figure 5-12: Motion Sequence of Robosnail 2 underside. The moving segments are shown in grey. Each of the five foot segments moves in succession; at the end of one cycle, the body moves forward by ΔL. The diagram is drawn assuming no back slip, in experiments, a certain amount of slip occurred so that the net translation after a cycle is slightly less than ΔL.

3 4, 1 2 3 4 5, [none], 1, ... (see Figure 5-12). Instead of the continuous motion of a real snail, where all points in the interwave are in actuality moving backwards in relation to the rest of the snail body, the interwave of Robosnail is stationary with respect to the body. When none of the wires are activated, the return springs restore the segments to their deactivated position. Controlling a backward movement for four of the platforms while simultaneously controlling the forward motion of the fifth would be unnecessarily complicated. The sequence of switching on the voltage for consecutive platforms is simpler while still keeping the necessary condition that the (n-1) feet are stationary with respect to the one foot in motion.

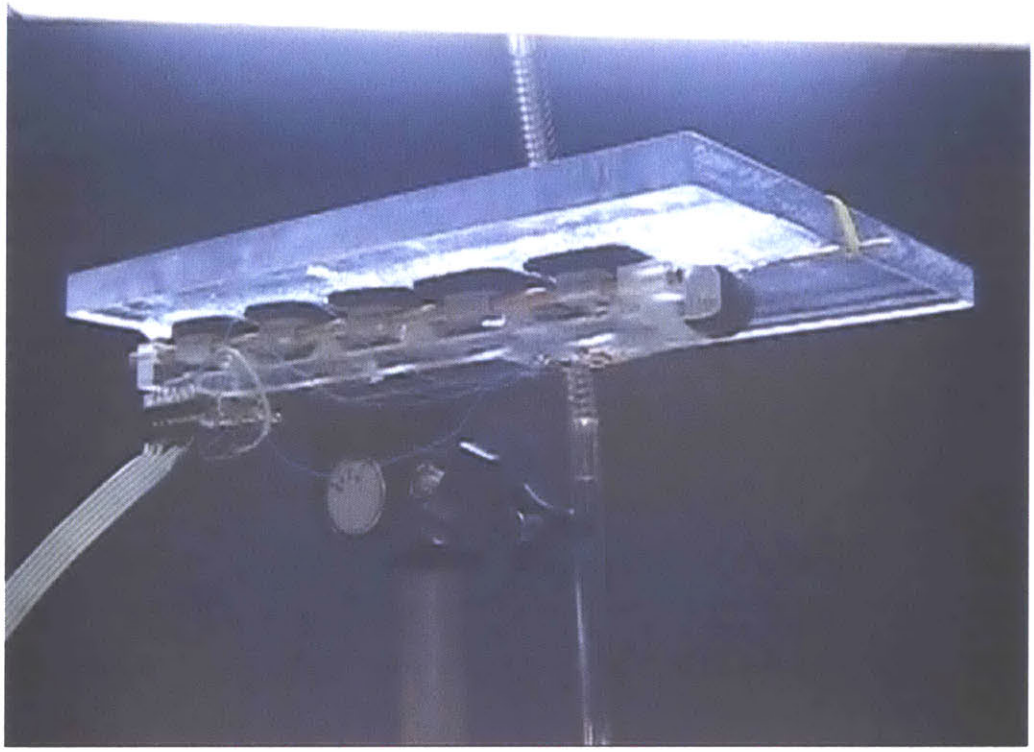

Figure 5-13: Experimental setup of Robosnail2 (video still). Here Robosnail 2 is inclined a full 180 degrees where it continues to move forward with ease.

5.4 Results

Robosnail 2 was tested on a tiltable platform covered in 1.5 mm thick layer of Laponite. The bulk of the Laponite was observed to keep its shape as a fixed layer on the platform as the robot slid along. This observation suggests that only a small layer of the Laponite touching the foot segment yielded into liquid form, while the rest remains in solid form. Robosnail 2 was able to climb Laponite-coated surface tilted at any angle, even in an inverted position, given the Laponite was of a sufficiently high concentration.

As the data shows, the motion per cycle is in all cases slightly less than the translation of one foot. Ideally the slip velocity should be zero and the snail velocity should be $\Delta L/T$ (this would be along the line $\frac{\Delta X/T}{\Delta L/T} = 1$). The slipping effect of the stationary sections can be explained by several phenomena: neither the Laponite layer nor the foam rubber of Robosnail foot sections was perfectly flat, therefore if the

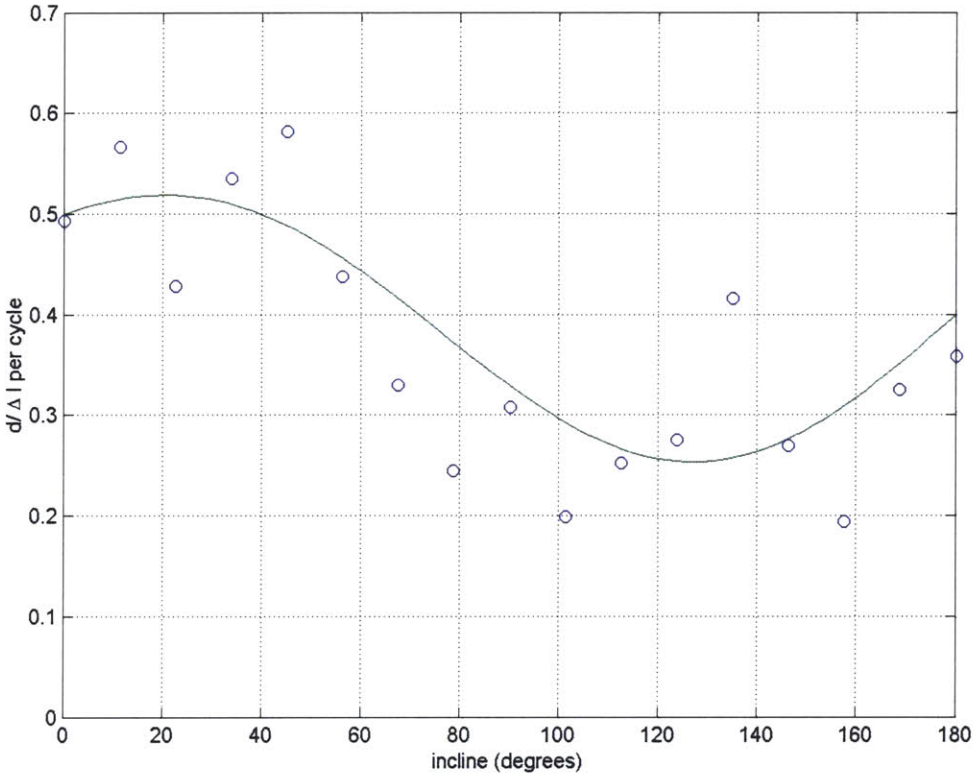

Figure 5-14: Distance-time plot of robosnail2 for various inclines. The curve $y = 0.05sin(\theta) + 0.1cos(1.3\theta) + 0.4$ is included as a plausible fit and bears no fundamental relation to theory.

moving section hits a lump or other imperfection in the Laponite, the resistant force of the moving section would be greater than $A\tau_y$, putting more force on the stationary sections and possibly causing the Laponite underneath to yield. Another cause for slippage is the Laponite under the stationary sections may have not had enough time to heal. This last problem could possibly be remedied by increasing the time of each cycle, to allow the Laponite to re-solidify at the expense of slowing down the translational speed of the snail. Finally, it was observed that there was delamination of the Laponite layer from the segments of the foot, decreasing the traction of the stationary foot segments. The most slip occurs between 60 and about 120 degrees, when the high angle of tilt decreased the normal force of the robot's weight and thus the traction. At high tilt, much of the adhesive force of the Laponite support both the weight of the snail and the viscous resistance of the moving foot section, while at near-flat angles near 0 and 180, the adhesive force mostly resists just the friction on the moving foot. We should expect a minimum displacement somewhere between 90 degrees and 180 degrees, where gravity works to decrease traction and to increase the resistive force of the weight, this is indeed supported by the data. Though there was some slipping at all angles of incline, Robosnail 2 consistently was able to exhibit forward motion at all inclined angles.

Chapter 6

Conclusion

6.1 Review

The three machines proved to be feasible swimmers in the low-Reynolds Number regime. The direction of motion predicted by the theory was confirmed in all cases by the experimental results.

The three-link swimmer does swim as was expected, in the same direction predicted by the simulations done by Becker et al. [10]. There still needs to be work done to numerically simulate a three-link swimmer composed of flat elements.

Robosnail 1 did not exhibit speeds as high as predicted by the theory, however the direction of motion and speed was found to be linear and proportional to wave speed, as predicted by the theory for low average height.

Robosnail 2 was highly successful, having proven its ability to climb a flat surface tilted at any angle including 180 degrees (full inversion). The Nitinol wire actuators were an ideal choice of actuator for their linear motion and high power-to-weight ratio. A high-concentration suspension of Laponite particles proved to be effective in adhering the snail to a flat surfaces. However, there was observed to be slippage at all angles, suggesting that the device and the fluid composition could be improved to decrease slippage and to increase the speed of the snail.

Future work involving these devices would require more detailed calculations of efficiency. The current three-link swimmer operates with its inner mechanism com-

pletely submerged in silicon oil the amount of dissipation caused by viscous friction between the lubricated parts would result in an expectedly low efficiency. Likewise, the number of planetary gear stages of Robosnail 1 (5 stages) and the mechanical friction between the aluminum plates and their guiding grooves must decrease the mechanical efficiency significantly. The efficiency of Robosnail 2 is the product of the efficiency of the muscle wires and the mechanical efficiency of the pulley and sliding foot sections.

6.2 Future designs

These three devices are only a small selection of the wide variety of possible ways to move through viscous fluid. S. Childress in his book *Mechanics of Swimming and Flying* [4] describes other possible motions specific to real microorganisms such as squirming, and several types of cilia motion (which can be analyzed much like wave-sheet swimming) and some motions not used by microorganisms such as toroidal rolling, where a toroidal animal continually turns itself inside out. Another similar hypothetical organism propels itself by generating peristaltic waves in an internal channel. Adjari [2] has derived a theory describing the motion of such an organism as a function of its internal wave speeds. An robot using this mechanism to move would be relatively simple to build, as most of it is a rigid structure except for the deformable inner channel.

Preliminary tests show that for a three-link swimmer of equal arm and body lengths, the use of flexible arms can increase the net translation per cycle to twice that of the case of motion using rigid arms. The effect of a flexing arms increases the asymmetry (with respect to time) of the motion - a flexible arm bends in a certain direction when rotating through a viscous fluid, but bends in the opposite direction when the angular motion is reversed. Apparently, this added asymmetry acts to increase the displacement per cycle, an effect worth looking into in greater detail. A related swimmer is G.I. Taylor's waving sheet swimmer - one possible design, which draws its central actuator design from Robosnail 1, would be to embed a rotating

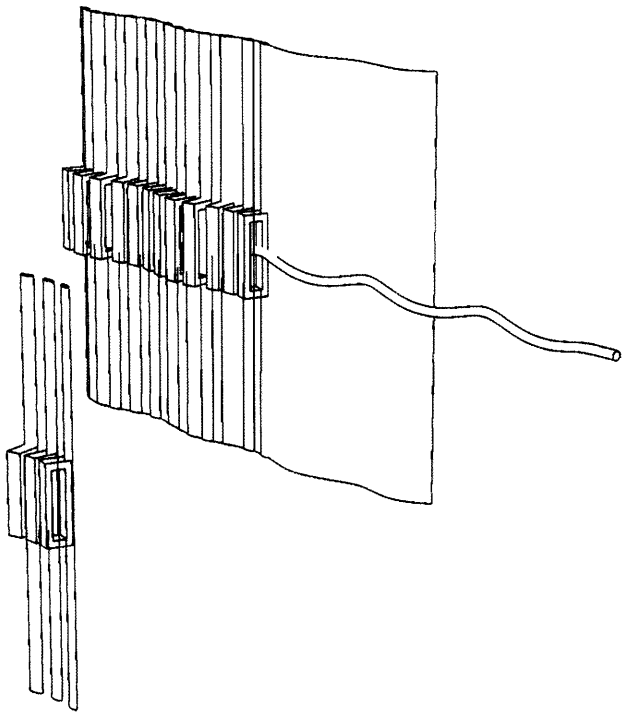

Figure 6-1: Waving sheet swimmer using rotating helix. The helix is threaded through a series of flattened openings attached to the sheet. When the helix is rotated, the traveling wave is generated.

helix inside of a hollow sheet one-way flexible sheet. Rotating the rod would deform the sheet in a sinusoid in the same was as Robosnail 1.

The research group of Prof. Thorsen is developing small thin PDMS devices with long interior channels. When a thin flexible channel is filled with fluid and a high pressure is applied, the flexible plastic expands enough that the surface is deformed. The device consists of a sheet with many such channels passing within. When the channels are activated in sequence, the flexible surface should deform in such a way as to create a traveling wave much like that generated by Robosnail 1. Figure 6-3 shows the approximate scale of the device developed by Thorsen et al.

One of the first problems to be solved is finding ways steering these devices. The two Robosnails and the three link swimmer currently are only capable of linear motion. For practical use self-contained robots, they will need ways of changing their direction of travel. A Robosnail 1 type robot can be given instead of one central

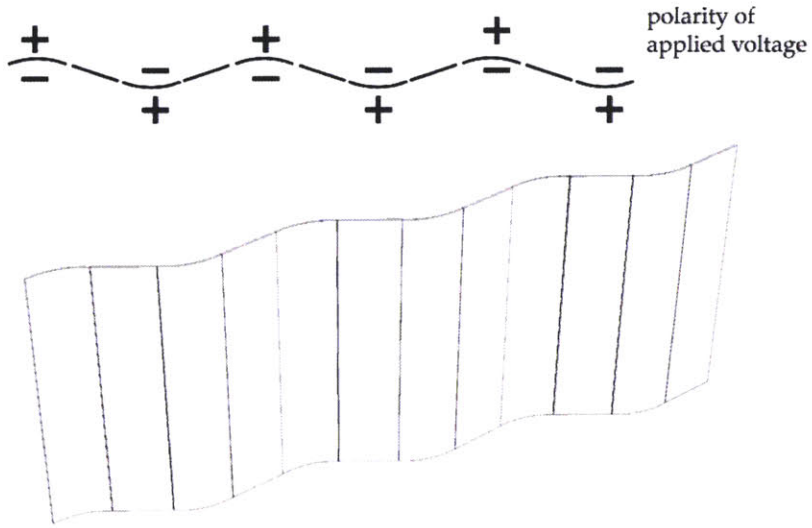

Figure 6-2: Waving sheet swimmer using electro-active polymer sheets. The direction of sheet bending depends on the polarity of applied voltage. using the proper phase of voltage, a traveling wave can be generated.

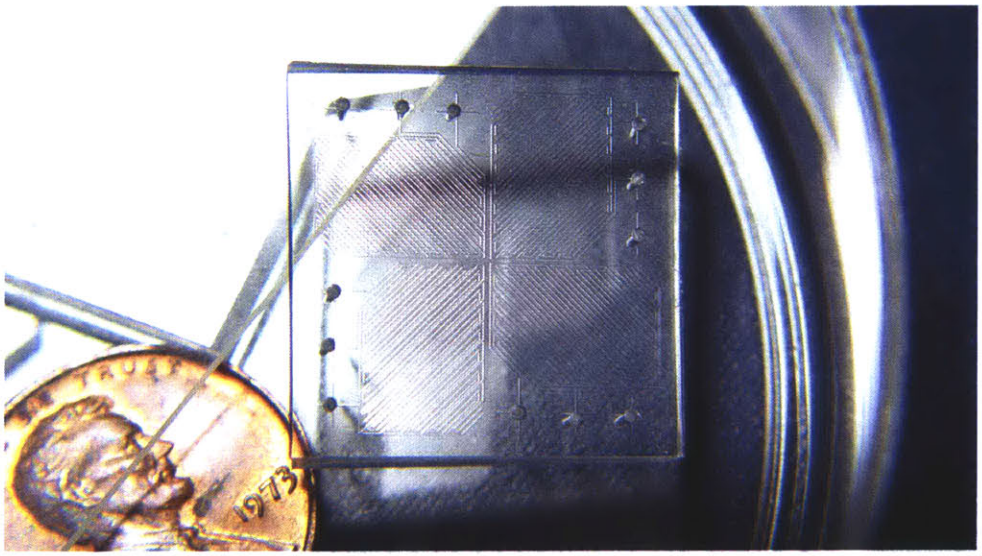

Figure 6-3: Three-phase expanding sheet micro-device inspired by Robosnail 1. Inflation of the long channels deforms the surface in a traveling wave, to transport a small flat object over a thin layer of PDMS using lubrication pressures.

helix, two independently controlled helices or it could have its foot split lengthwise into two independently controlled sections.

The current robosnails use external power sources to save on weight, but fully autonomous versions will need to use self-contained battery or other power source and carry and secrete its own supply of lubricating fluid.

The designs presented in this thesis lend themselves to the use of new actuators. In the three-link swimmer and Robosnail 1, a motor or spinning cam was still the basis of the mechanical motion, but in the case of Robosnail 2, linearly acting muscle wires were used to move the feet. Future versions of this type should aim for a more integrated design. The Electro-active polymers are another option- promising because they exhibit very high strains where the muscle wires change length by only up to 8 percent when activated.

Electrically activated curving polymer sheets could be cut into narrow strips and attached in segments to create a long sheet. Activating separate segments to bend in various directions in the proper sequence should be able to create a traveling wave in the sheet a like Taylor's wave swimmer and Robosnail 2. A sheet of this material could be used to wrap an arbitrary shape, and when the sheet is set in motion, the effect should be similar to that of a surface covered in beating cilia.

Similarly, polymers which contract with an electrical charge can be attached end-to-end and a voltage applied to specific bands, more accurately simulating the continuous motions of a snail's muscular foot. The flexibility of the this kind of sheet would allow it to be backed by a secondary layer of bending actuators, allowing it to conform actively to the substrate.

Another related topic deserving attention is optimization of the synthetic mucus by exploring the optimal concentration of Laponite and water. Instead of using a simple Laponite-water solution as a lubricating layer, the effect of the addition of polymers should be tested. Snail mucus exhibits a certain amount of viscoelasticity. The presence of polymer chains in the mucus may allow more elastic deformation of the layer before shearing, increasing the safety zone of the snail's operation - it would be less sensitive to sudden jolts or small variations of the foot deformation which

might de-solidify a Laponite layer, but only elastically deform a layer of snail mucus.

It would be worthwhile to study motion through other non-Newtonian fluids such as granular fluids, shear-thickening fluids: a robot built like Robosnail 2 should move in the opposite way as the current version in a shear thinning fluid. Because a newtonian fluid is the neutral case where Robosnail 2 undergoes no net translation per cycle, and Laponite causes forward motion, the effect of a shear thickening fluid such as custard should cause the opposite effect - backwards motion.

In the near future we hope to explore these possibilities and their potential for application.

Bibliography

[1] Laponite- synthetic layered silicate- its chemistry, structure, and relationship to natural clays. Technical report, Rockwood Additives Limited, Moorfield Road, Widnes, Cheshire WA8 0JU, UK.

[2] Armand Ajdari and H.A. Stone. "A note on swimming using internally generated traveling waves". *Physics of Fluids*, 11:1275–1277, 1999.

[3] D. Bonn, P. Coussot, HT Huynh, F. Bertrand, and G. Debregeas. "Rheology of soft glassy materials". *Europhysics Letters*, 59:786–792, 2002.

[4] S. Childress. *The Mechanics of Swimming and Flying.* Cambridge University Press, Cambridge, 1997.

[5] M. Denny. "A quantitative model for the adhesive locomotion of the terrestrial slug, *Ariolimax columbianus*". *Journal of Experimental Biology*, 91:195–217, 1981.

[6] M. Denny. "Mechanical properties of pedal mucus and their consequences for gastropod structure and performance". *American Zoology*, 24:23–36, 1984.

[7] M. Denny. "Invertebrate mucous secretions: functional alternatives to vertebrate paradigms". *Journal of Experimental Biology*, pages 337–366, 1989.

[8] AI Dobrolyubov and G Douchy. "Peristaltic transport as the travelling deformation waves". *Journal of Theoretical Biology*, 219:55–61, 2002.

[9] R.G. Gilbertson. *Muscle Wires Project Book.* Mondo-Tronics, 2000.

[10] Becker L.E., Koehler S.A., and H.A. Stone. "On Self-Propulsion of Micro-Machines at Low Reynolds Number: Purcell's Three-Link Swimmer". *Journal of Fluid Mechanics*, 490:15–35, 2003.

[11] E.M. Purcell. "Life at Low Reynolds Number". *American Journal of Physics*, 45:3–11, 1977.

[12] DD Spain and WM Kier. "Peristaltic locomotion in holothuroids (Echinodermata)". *Integr. Comp. Biol*, 42:1316–1316, 2002.

[13] N Willenbacher. "Unusual Thixotropic Properties of Aqueous Dispersons of Laponite RD". *Journal of Colloid and Interface Science*, 182:501–510, 1996.